ADVANCED HEALTHCARE MATERIALS
www.advhealthmat.de

3D Bioprinting of Lignocellulosic Biomaterials

Amin Shavandi, Soraya Hosseini, Oseweuba Valentine Okoro, Lei Nie,* Farahnaz Eghbali Babadi, and Ferry Melchels**

The interest in bioprinting of sustainable biomaterials is rapidly growing, and lignocellulosic biomaterials have a unique role in this development. Lignocellulosic materials are biocompatible and possess tunable mechanical properties, and therefore promising for use in the field of 3D-printed biomaterials. This review aims to spotlight the recent progress on the application of different lignocellulosic materials (cellulose, hemicellulose, and lignin) from various sources (wood, bacteria, and fungi) in different forms (including nanocrystals and nanofibers in 3D bioprinting). Their crystallinity, leading to water insolubility and the presence of suspended nanostructures, makes these polymers stand out among hydrogel-forming biomaterials. These unique structures give rise to favorable properties such as high ink viscosity and strength and toughness of the final hydrogel, even when used at low concentrations. In this review, the application of lignocellulosic polymers with other components in inks is reported for 3D bioprinting and identified supercritical CO_2 as a potential sterilization method for 3D-printed cellulosic materials. This review also focuses on the areas of potential development by highlighting the opportunities and unmet challenges such as the need for standardization of the production, biocompatibility, and biodegradability of the cellulosic materials that underscore the direction of future research into the 3D biofabrication of cellulose-based biomaterials.

1. Introduction

Over the last decade, complex and heterogeneous structures with various mechanical and biological properties have been developed using 3D biofabrication techniques. 3D biofabrication has been researched for application in orthopedics, spinal surgery, maxillofacial surgery, neurosurgery, and cardiac surgery.[1] The technological advancement resulted in different types of 3D printing modalities based on jetting, extrusion, and photopolymerization; ranging from basic configurations to more advanced systems with high resolution and comprising several modalities and materials.[2] Also, several printable inks with different physiochemical properties have been developed for 3D printing on different devices (**Figure 1**).[3] To fabricate structures containing cells, a straightforward approach is first to 3D print the structure using a biomaterial ink and then seed the cells into the surface of the material. For a more complex cellular organization the cells need to be contained in ink; however, developing such a "bioink" is not a straightforward task.[4] The cells' encapsulation, survival during the preparation, and printing and tuning the cells function in the structure after printing are significant challenges.[5] Properties such as rheology, shrink resistance, and the capability to form stable networks are major criteria for establishing the suitability of inks for 3D printing. At the same time, low polymer concentrations and low crosslink densities are

Dr. A. Shavandi
BioMatter–Biomass Transformation Lab (BTL), École Polytechnique de Bruxelles
Université Libre de Bruxelles
Avenue F.D. Roosevelt, 50-CP 165/61, Brussels 1050, Belgium
E-mail: amin.shavandi@ulb.ac.be
Dr. S. Hosseini
Department of Chemical Engineering
National Chung Cheng University
Chiayi 62102, Taiwan
Dr. O. V. Okoro
Department of Process Engineering
Stellenbosch University
Private Bag X1 Matieland 7602, South Africa
Dr. L. Nie
College of Life Sciences
Xinyang Normal University
Xinyang 464000, China
E-mail: ielei@xynu.edu.cn
Dr. F. Eghbali Babadi
Bio-Circular-Green-economy Technology & Engineering Center
BCGeTEC
Department of Chemical Engineering
Faculty of Engineering
Chulalongkorn University
Phayathai Road, Bangkok 10330, Thailand
Dr. F. Melchels
Institute of Biological Chemistry, Biophysics and Bioengineering
School of Engineering and Physical Sciences
Heriot-Watt University
Edinburgh EH14 4AS, UK
E-mail: F.Melchels@hw.ac.uk

The ORCID identification number(s) for the author(s) of this article can be found under https://doi.org/10.1002/adhm.202001472

DOI: 10.1002/adhm.202001472

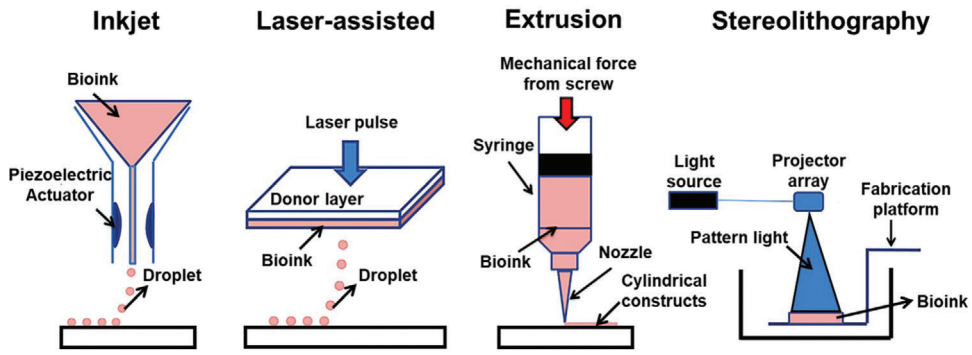

Figure 1. Bioprinting techniques. Inkjet deposits the ink using a piezoelectric actuator; in laser-assisted method, the laser stimulates an energy-absorbing donor layer coated with the ink which creates bubbles at the interface of the ink layer resulting in its deposition in the form of droplets; in extrusion mechanical force use to deposit the ink, and in stereolithography exposure of a light-curable resin to a precise source of light with a patterned binary image result in the 3D structure.[11] Adapted with permission of a creative commons license.[] Copyright 2019, the Authors. Published by Hapres Co., Ltd.

required to not restrict the encapsulated cells from driving tissue maturation.[6] This is where lignocellulosic materials come into view, as their insoluble nanostructures can improve printability and gel stability even at very low concentrations. While many articles have published on 3D bioprinting, most of these articles have focused on using well-known polymers such as alginate and gelatin toward new applications, while less attention has been paid to developing new ink materials. In order to simulate the complex mechanical and biological profile of the natural tissue, accessing different ink materials with tunable physicochemical properties is essential. It is essential to highlight that "bioink" are printable materials that contain cells as a mandatory component and therefore formulations containing biologically active molecules or components without any cells, does not consider as a bioink. These aqueous formulations of printable materials or precursors of hydrogels that containing biological factors therefore are quantifies as "biomaterial inks."[4] However, as long as they are used "in order to produce bioengineered structures serving in regenerative medicine, pharmacokinetic and basic cell biology studies," the 3D printing of either type of ink is termed 3D bioprinting.[7]

In recent years there has been an increasing interest in exploring the potential of lignocellulosic materials for 3D biofabrication. Cellulosic materials are biocompatible, with high surface area (a few hundreds of $m^2\ g^{-1}$),[8] low density, high tensile strength, and elastic modulus (≈100 GPa for single cellulose fibrils).[9] In this regard, there is a rapidly growing body of knowledge on wood-based products, and there are several comprehensive articles on the cellulosic-based materials and their biomedical applications.[10] Given the exponential growth of research on lignocellulosic materials in the field of biomaterials, this review paper seeks to present discussions covered in articles mainly published in the last three years related to the current state of 3D bioprinting of the lignocellulosic based materials. The review simultaneously discusses the significant parameters to consider for 3D bioprinting of these materials for diverse biomedical applications. We discuss the different sources of lignocellulosic materials for biofabrication, their physiochemical properties, and provide extensive discussion on lignocellulose-based 3D biofabricated materials. Finally, this review attempts to ascertain what are the primary consideration, challenges, and emerging techniques in using lignocellulosic materials for 3D biofabrication for biomedical applications.

2. Types and Sources of Lignocellulosic Materials

2.1. Cellulose

Plant cellulose, the most abundant polymer in nature, is a semicrystalline, highly polymerized natural homopolymer with reinforcing effect in wood and nonwood fibers.[12] Cellulose is a linear polymer consisting of β-D-glucose units with β-1,4-glucan bonds, which are formed due to condensation reactions that occur between an OH group of the α-anomeric form of C_1 atom and the C_4 carbon atom of other molecules[13] (**Figure 2**A). The cellulosic fibers in wood exist as 3D matrixes, with these 3D matrixes responsible for its crystalline form and resulting mechanical properties.[14] Like cellulose, β-glucans also consist of long chains of glucose molecules linked with β bonds and can be found inside the cell wall of bacteria, fungus and yeasts. However, β-glucans differ from cellulose in having branched chains besides the straight linear chains. Where cellulose consists of linear chains (unbranched) that are laid crowded together, the rings in beta-glucan contribute to making "kinks" to generate the molecule in a cylindrical shape. As a result, β-glucans are soluble fibers due to having both branched and linear linkages that water can easily diffuse into the network and solubilize them, whereas cellulose with its high molecular weight, strong hydrogen bonding between the molecules and crystalline structure is water-insoluble.[15]

Cellobiose is produced by hydrolysis of cellulose. The structural cellobiose is a disaccharide (two β-glucose molecules $C_{12}H_{22}O_{11}$) in which the adjacent glucose residues are rotated 180° with respect to each other. The glucose molecules are individually linked to each other via two hydrogen bonds. Glucose units contain equatorial and axial hydroxyl groups in which an axial hydroxyl group is more reactive than an equatorial hydroxyl group. Also, equatorial hydroxyl groups are radially placed away from the ring (pyranose), while the axial hydrogen atoms are aligned perpendicular to the ring. The source and synthesis

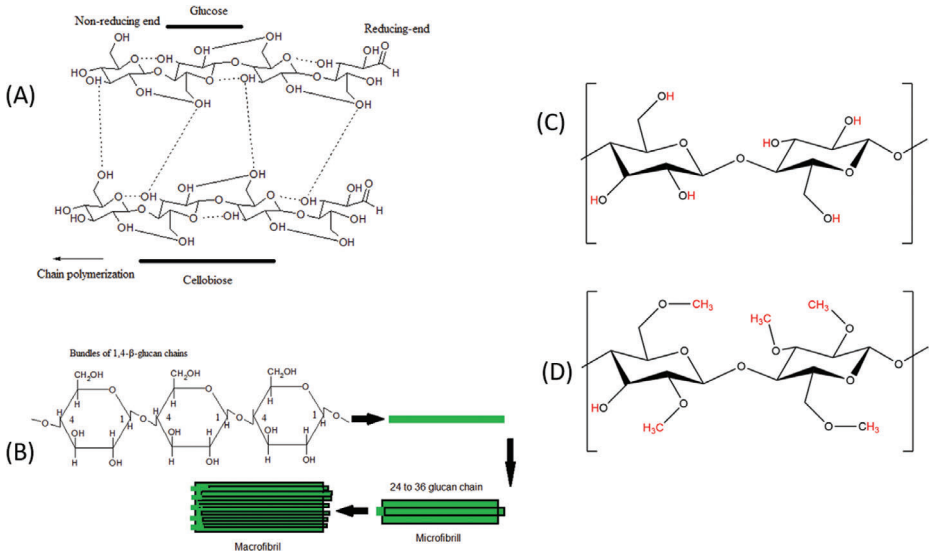

Figure 2. A) Glucan chains (glucopyranose rings), the inter- and intrachain hydrogen bonding in cellulose. B) Bundles of β-1,4-glucan chains. C) Schematic of cellulose and D) methylcellulose where methyl groups substitute the hydrogen atoms.[43]

conditions affect the number of glucose units that can be used for determining the degree of polymerization in a cellulose chain.[16] Individual glucan chains in cellulose are comprised of two sides in which the free C_1 hydroxyl group is known as the reducing end while the nonreducing end is located on the opposite side as the free C_4 hydroxyl group (unmodified), with the possibility to be modified via chemical methods. The nonreducing part of molecules is active for the adjunction of new glucose to extend individual chains in a cell.

Approximately 6–8 glucan chains are assembled parallel to each other to form the subelementary fibrils (protofibrils) with a diameter ranging from 2 to 20 nm depending upon the source. The aggregation of elementary fibrils is stabilized via a combination of van der Waal's forces, and inter- and intramolecular hydrogen bonds. These fibrils gather into long microfibrils to form tight ribbons (Figure 2B). The type of organism and enzyme involved in the biosynthesis affect the shape, size, and organization of the microfibrils. These factors determine the degree of crystallinity of cellulose, and as a result, mechanical strength.

2.1.1. Cellulose Nanocrystal, Nanofibril, and TEMPO Oxidized Cellulose

An extensive review of the literature suggests that the major forms of cellulose employed in the medical field are cellulose nanocrystals (CNC), micro/nano fibrillated cellulose (MFC and NFC) and bacterial cellulose (BC). **Table 1** summarize names, sources and some properties of nanocelluloses. CNC and NFC are nanoscale cellulose fibers that present reinforcing effects in polymer nanocomposites[17] with NFC is shown to consist of both amorphous and crystalline regions compared to CNCs which contains only crystalline regions.[18] The structure of bacterial cellulose is different due it being expressed in microorganisms, as discussed in more detail in Section 2.1.

According to Lin et al.,[19] CNC and NFC are typically produced via chemically induced destruction strategies (i.e., acid hydrolysis) and mechanically induced destructuring strategy (i.e., grinding) respectively. The hydrolysis facilitates the removal of amorphous segments in the cellulose fibers. CNC have a crystalline morphology which is characterized by high aspect ratio, high surface area, and high mechanical strength. When CNC is obtained via acid hydrolysis, the surface of CNC will be negatively charged, thus promoting its dispersion in water due to electrostatic repulsions.[20] The magnitude of the surface charges correlates with the severity of the hydrolysis condition[21] and thus CNCs may exhibit amphiphilic properties. The amphiphilic nature of CNCs suggests that CNC can also act as a stabilizers in emulsions and foams.[22] If the acid used in hydrolysis is sulfuric acid or phosphoric acid, the derived CNC will be characterized by a chiral nematic structure.[20] If on the other hand, hydrochloric acid is employed in the hydrolysis process, prior to a post reaction sulfonation will generate CNC characterized by a birefringent glassy phase.[20] CNCs are typically presented as elongated rod-like (or needle-like) nanoparticles, such that each rod exists as a rigid cellulosic crystal,[19] thus having the potential to serve as reinforcing agents in polymer nanocomposites.

NFCs consist of individual and aggregated nanofibrils which are composed of both crystalline and amorphous cellulose regions, thus resulting in its less rigid structure compared to CNCs. To prepare the cellulose nanofibrils (CNF), mechanical fibrillation of cellulose biomass is undertaken. This mechanical fibrillation may be achieved via homogenization, microfluidization, or ultrafine grinding of cellulose.[23] In some cases, the CNF may be subjected to enzymatic, chemical, or mechanical pretreatments to reduce energy input and enhance CNF quality.[23] CNFs are typically characterized by lateral dimensions of 3–10 nm and a length of 0.5–2 µm,[24] by high intrinsic properties with a strength of 1–3 GPa, a low density of ≈1.5 g cm^{-3}, and a crystal modulus of 138 GPa.[24]

MFC consists of long, flexible, and entangled cellulose nanofibers and are characterized with lateral dimensions in the nanoscale range and lengths up to the micron scale. MFCs are characterized by a fiber structure that resembles both water-

Table 1. Common cellulosic materials: types, synonyms, common production methods, typical dimensions, and crystallinity.[9,30].

Type of cellulose	Synonyms	Production method	Typical size and crystallinity
Cellulose nanocrystal (CNC)	Nanocrystalline cellulose (NCC), crystallites, cellulose whiskers, cellulose nanowhiskers rod-like cellulose	Acid hydrolysis of cellulose from many sources such as wood, cotton, hemp, flax, wheat straw, mulberry bark, ramie, Avicel, tunicin, cellulose from algae, and bacteria diameter: 5–70 nm length: 100–250 nm (from plant celluloses) 100 nm to several micrometers (from celluloses of tunicates, algae, bacteria)	High aspect ratio (3–5 nm wide, 50–500 nm in length), are 100% cellulose, highly crystalline (54–88%), rod-like or whisker, length 0.05–0.5 μm, width 3–5 nm, height 3–5 nm
Microcrystalline cellulose (MCC)	Cellulose microcrystals (CMC), one brand name is Avicel	Acid hydrolysis of wood fiber from various sources including wood pulp and purified cotton linters back-neutralization with alkali, and spray-dried	Highly crystalline, length 10–50 μm, width 10–50 μm, height 10–50 μm
Nanofibrilated cellulose (NFC)	Cellulose nanofibrils/fibers (CNF)	Mechanical processes: high-pressure homogenizers, grinders, cryocrushing, and microfluidization high intensity ultrasonic treatments,	A high aspect ratio (4–20 nm wide, 500–2000 nm in length), 100% cellulose and contain both amorphous and crystalline regions MFC and NFC terminologies are sometimes used interchangeably in the literature, length 0.5–2 μm, width 4–20 nm, height 4–20 nm
Microfibrillated cellulose (MFC)	Cellulose microfibrils (CMF)	Delamination of wood pulp by mechanical pressure before and/or after chemical or enzymatic treatment	Contains both amorphous and crystalline regions, length 0.5–10's μm, width 10–100 nm, height 10–100 nm
Bacterial cellulose (MBC)	Bacterial nanocellulose, microbial cellulose, biocellulose	Synthesis of aerobic bacteria such as acetic acid bacteria of the genus *Gluconacetobacter*	Morphology depending on the specific bacteria and culturing conditions. length >1, width 30–50 nm, height 6–10 nm

soluble polymers and insoluble additives, thus contributing to its versatility as a biomaterial composite.[25] These MFCs may be prepared by applying high-pressure homogenizing action on a dilute slurry of cellulose fibers, leading to the disintegration of the fibers to expose their substructural microfibrils.[26] These MFCs are only moderately degraded although their surface areas are greatly expanded.[25]

TEMPO oxidization refers to 2,2,6,6,-tetramethylpiperidine-1-oxyl mediated oxidation and is applied to selectively oxidize C6-primary hydroxyls exposed on the cellulose microfibril surfaces into C6-carboxylate groups in water.[27] The generation of these negatively charged C6-carboxylate groups will facilitate the weakening of the interfibrillar hydrogen bonds, due to the electrostatic repulsions produced by negative charges and thus enabling the disintegration of oxidized fibers into individualized cellulose nanofibrils.[27] The individual fibers, obtained after TEMPO oxidization are characterized by widths ranging from 3 to 4 nm widths and high aspect ratios (>50).[28] The fibers are also long in length, tensile strengths (200–300 MPa), elastic moduli (6–7 GPa), high light transparencies and flexibilities.[29] These aforementioned properties of the TEMPO-oxidized cellulose enhance its tenability.[29b]

2.1.2. Methylcellulose

Methylcellulose is an ether derivative of cellulose that is produced through partial substitution of hydrophilic hydroxyl groups of cellulose with hydrophobic methoxy groups.[31] MCs can be prepared via a Williamson ether synthesis process which involves the employment of an alkali–metal salt of the hydroxy compound and an alkyl halide, in organic solvents or under the action of phase-transfer catalysts.[32] Methylcellulose can also be prepared via heterogeneous media with methyl chloride and may be synthesized from dimethyl sulphate and methyl iodine using suitable apparatus and processes.[33] Methylcellulose is biocompatible and has been used as food and drug additive in many countries.[34] MCs soluble in cold water but insoluble in hot water, with increasing viscosity observed as temperature increases, such that gel formation occurs at a temperature of 50–55 °C.[35] In the sol state, MC is hydrophilic, but its hydrophobic properties increase due to the gelation process.[36] This gelation process is fully reversible.[37] Its thermal gelation properties and its solubility promotes its utilization in pharmaceutical industry as a disintegrant for the sustained release of pharmaceutical bioactive compounds from tablets.[38] MCs, despite cellulose, CNC and CNF are soluble in aqueous solution. The ordered hydrogen bonds between hydroxyl groups of the cellulose molecules are disturbed by the methoxy groups, which allows the water molecules to penetrate the MC structure and form electrostatic bonds with the polar side chains.[39] Nevertheless, due to the nonpolarity of methoxy groups, increasing the degree of substitution (DS) eventually decrease its solubility in aqueous media. For that reason, the degree of substitution of MC for tissue engineering applications is below 2.5, and usually a DS in the range of 1.5–1.9 is considered optimal for solubility. MC with a DS of 2.5–3.0 is soluble in polar organic solvents.[39] The high binding affinity between the polar MC and molecules of water results in a viscous hydrogel network, which is essential for its bioprinting applications.[37] The gel strength and temperature of gelation depend on the DS, con-

centration, molecular weight, and concentration of electrolytes. The gelation temperature decreases as DS and MC concentration increase, while increasing the molecular weight improves the strength of the gel.[40] Increasing the ionic strength, for example, through the addition of salts in the aqueous media, can affect the temperature of gelation and gel strength in either direction. Methylcellulose as a thermal gelling polymer has mainly been used in 3D printing as a blending material with other polymers such as alginate[41] and hyaluronic acid[42] to improve the printing process of these polymers. Readers are referred to the review articles[34] regarding the recent development in applying methylcellulose for 3D printing for biomaterials engineering.

2.1.3. Microbial Cellulose

Although plants are mostly considered the primary source of cellulose, cellulose can be produced from various bacteria as an alternative source. There are some microorganisms (bacteria, tunicates, algae, sponge, or fungi) that are able to produce cellulose, known as microbial cellulose (MBC).

Bacteria can produce MBC (which can then also be referred to as bacterial cellulose (BC)) through oxidative fermentation in both nonsynthetic and synthetic medium. The ultrathin 3D network of MBC nanofibers (pellicle) is formed in parallel to the medium surface via Intra- and intermolecular hydrogen-bonding network, van der Waals and hydrophobic interactions. BC is an exopolysaccharide made up of β-1,4-D-glucopyranose units which are interlinked by intermolecular hydrogen bonds with the molecular formula of $(C_6H_{10}O_5)_n$.

In contrast to plant-derived celluloses, MBC is free from lignin, hemicelluloses, and pectin and there is no need to use a harsh process chemistry such as acid hydrolysis and alkaline delignification in order to carry out the purification processes; thus, MBC purification can be carried out easily with a low energy process. Furthermore, MBC has shown to possess higher crystallinity (70–80%), purity, high-water holding capacity (99%), a high degree of polymerization (up to 8000), good mechanical strength (>2 GPa), unique nanostructure, and nontoxicity in compared to plant cellulose, while also retaining its biocompatibility.[44] Typically, a ribbon of bacterial nanofibril has a width of about 60 nm with indefinite length, while softwood pulp fibers are normally at least 100 µm wide. Due to this fibril thickness, MBC has around 200 times higher surface area compared to softwood pulp fibers. This high surface area and capabilities for hydrogen bonding make BC able to retain up to 700% water.[45]

That said, MBC has attracted much attention for various applications including for 3D biofabrication. Different types of bacteria generate MBC with different structures, morphology, properties, and applications. Generally, *Aerobacter*, *Alcaligenes*, *Achromobacter*, and *Pseudomonas* (flocculation in wastewater); *Rhizobium*, *Agrobacterium* (attachment to plants); *A. hansenii*, *Acetobacter* (Maintenance aerobic environment); *Gluconacetobacter* (Aerobic environment), *Gluconacetobacter xylinus* , *Sarcina*, *Azobacter*, and *Zoogloea* are known as bacteria sources which can produce BC with favorable physical properties for diverse applications in the biomedical field, e.g., artificial skin, wound dressing, tissue-engineered blood vessels, vascular grafts cartilage replacement, tissue and bone regeneration, and medical pads and dental implants.[46]

Among all types of the MBC producing bacteria, *G. xylinus* (formerly *Acetobacter xylinum*) are widely used sources.[47] *A. xylinum* with high MBC productivity has been used commercially for producing MBC. These bacteria can polymerize up to 200 000 glucose molecules per second using cellulose synthase.[48] MBC synthesis can be categorized into two intermediary steps as following: i) the intracellular formation of 1,4-β-glucan chains and ii) the assembly and crystallization of cellulose chains. MBC starts to generate when the present bacteria polymerize the glucose residues into linear β-1,4-glucan.

Notwithstanding all its advantages, the MBC production process is relatively costly due to the utilization of expensive culture media.[49] Therefore, a cost-effective culture medium is the most important hurdle and has attracted interest from many researchers. Various byproducts from dairy, fruit juices, textile industries, wine fermentation waste broth, starch waste, biodiesel byproducts, confectionery industries, etc., have been proposed as media for MBC production.[50]

In order to develop MBC materials with desirable biological, mechanical, physical, magnetic, and conducting properties, MBC-based composites have been established based on impregnating nanomaterials, metals, metal oxides, and polymers as additives in MBC matrix. Although potentially applicable to other forms of lignocellulosic materials as well, various successful attempts were carried out specifically on MBC to include antimicrobial activity. Several methods such as the inclusion of, or modification with antibacterial peptides,[51] silver nanoparticles,[52] in situ synthesis of SiO_2 coated Cu nanoparticles,[44b] and antiseptics such as povidone–iodine and polyhexanide,[53] tetracycline hydrochloride (TCH)-loaded bacterial cellulose,[54] antibiotic fusidic acid,[46c] grafting of ammonium moieties (3-aminopropyl)-trimethoxysilane,[55] aminosilanes,[56] and nano-ZnO[57] have been investigated to impart MBC with antimicrobial properties. MBC modifications in order to improve properties can be carried out through two methods of ex situ chemical treatments (carboxylation, acetylation, amidation, or incorporation of nanomaterials) and in situ biotreatments. The ex situ MBC modifications are generally performed after the MBC has produced using physical methods or hazardous chemicals and solvents which can result in some issues related to environmental toxicity. Unlike this method, in situ MBC modifications can reduce the problems and open new researches in biomedical applications. using the in situ modification method it is possible to changing the resulting MBC by modifying the bacterial cell culture such as changing the source of carbon or adding additives such as reinforcing materials. Glucose as a carbon source is mostly used for in situ MBC methods. However, the utilization of biomass sources is encouraged due to consider economics and environmental concerns.[58]

2.2. Hemicellulose

Hemicelluloses (xylans) are the second most abundant group of polysaccharides providing the structural strength of plants, through a complex crosslinking/bonding network with cellulose and lignin.[59] The macromolecule of hemicellulose consists of

complex branched heteropolymers that form hydrogen bonding with cellulose and form covalent bonding with lignin via α-benzyl ether linkages, and form ester linkages with acetyl units and hydroxycinnamic acids.[60] These bonds tend to limit the hemicellulose liberation from the matrix of the cell wall.[60] Hemicellulose is composed of hexoses (C_6) of D-galactose, L-galactose, and D-mannose and L-fructose and pentoses (C_5) of L-rhamnose, arabinose, and xylose. It also contains D-glucuronic acid and acetylated sugars.[61] Biorefineries can separate hemicelluloses from wood through environmentally acceptable processes such as hot water extraction. Hemicelluloses in hardwoods are large xylans and in softwood, glucomannans. In plant cell wall structure, hemicelluloses are in a firm bonding with cellulose fibers. This affinity between cellulose and hemicellulose is preserved after wood being processed in biorefineries which makes hemicellulose an important material for modification of cellulose fibers.

2.3. Lignin

One of the main components of the plant cell wall is lignin, which can significantly enhance the mechanical strength of cells. Lignin constitutes the third major component of wood. It is a complex aromatic copolymer network,[62] having a 3D structure build from the main monomers *p*-coumaryl, sinapyl, and coniferyl alcohols. Combined with the presence of many functional groups, e.g., hydroxyl, phenolic hydroxyl, aliphatic hydroxyls, sulfonic, methoxyl and carboxyl groups, tensile properties, and antioxidant activity. Wood lignin exists mainly as β-O-4′ alkyl-aryl ether substructures, minor amounts of β–5′ (phenylcoumarans, 6%) and other condensed substructures.[63] According to Lochab et al.,[64] the macromolecule of lignin is rich in phenolic derivatives such as cresol, catechol, guaiacols, syringol, and eugenol, thus possibly serving as a sustainable source of useful high-value phenolic polymers.

3. Biofabrication Using Cellulosic-Based Biomaterials

3.1. Cellulose Nanocrystals and Nanofibers

Recognizing the properties of cellulose fibers, extensive studies have been undertaken over the last decade, specifically in the production of hydrogels using native cellulose, cellulose nanowhisker, nanocrystals (CNCs), cellulose nanofibrils, nanofibers (CNFs), and cellulose derivatives such as hydroxypropyl methylcellulose. These cellulose fibers have also been employed in 3D printing, with the most common native cellulose-based 3D printing material being the cellulose nanofibrils (CNF) hydrogel (**Table 2**).[65] The cellulosic materials concentration and the applied shear rate have been demonstrated to influence alignment of anisotropic particles during the ink deposition.[66] These materials can also increase viscosity of the ink which will lead to higher printing fidelity although significantly higher viscosities increase shear stress, during the ink application.[67]

The extensive use of cellulose nanofibrils (CNF) hydrogel was highlighted in ref. [10d] where the functionality of the employment of CNF in drug delivery, wound dressings, and the development of tissue engineering scaffolds was extensively discussed. Additionally, the prospects and ongoing challenges of CNC- and CNF-based hydrogels for biomedical applications were summarized. The work presented in[10d] demonstrated that CNC- and CNF-based hydrogels are promising for diverse biomedical applications. 3D printing of cellulose is mostly used in combination with other polymers including alginate,[68] gelatin,[69] methacrylated gelatin, hyaluronic acid, and PLA[42,68–70] and is being studied as a viable route to fabricated 3D structures for tissue engineering applications.

Crosslinking of cellulosic polymers to form printable hydrogels is a critical aspect of using these compounds for 3D biofabrication. Leppiniemi and co-workers were able to establish the possibility of employing $CaCl_2$ as the crosslinker for a mixture of alginate, TEMPO-oxidized cellulose nanofibrils (TCNF) and glycerin to develop 3D-printable bioactivated hydrogels suitable for wound healing applications.[71] The bioactivated hydrogel developed was later functionalized covalently via the attachment of the tetrameric biotin-binding protein of avidin which enhanced the material stability. Leppiniemi and co-workers also stated that opportunities for further functionalization via interactions between avidin and biotin interactions existed largely due to the stability of the neutralized chimeric avidin. Increasing the share of a strength additive such as CNF in the ink formulation can minimize shrinkage and reduce the collapsing of the printing paste.

Heggset et al. evaluated the printability of hydrogels based on cellulose and alginate, thereby focusing specifically on the potential effect of alginate source.[72] Although the source does not affect the viscoelastic properties it does play an essential role in the mechanical properties of the inks (CNF, CNC, or the mixture) for 3D bioprinting. Comparing the alginates from *Macrocystis pyrifera* and *Laminaria hyperborean*, the latter was reported as a better choice when high mechanical strength is required, also showing lower syneresis. Knowing that alginate has low viscosity and to improve the shape fidelity, CNF was added to the mixture. The material with 4% CNF was printable with suitable shape fidelity while replacing CNF with CNC negatively affected the shape fidelity of the material due to a reduced complex viscosity. Therefore, CNC can be used to improve the total content of the ink without increasing the viscosity and, without obstructing the printing and the force needed for the extrusion. The same group in 2017[73] reported the high rupture strength, compressibility, and gel rigidity of CNF and alginate hydrogels. Therefore, printable hydrogels with 130–150 kPa Young's modulus and 1.5–6 kg cm^{-2} rupture strength can be formulated by tuning the amount of CNF and type of alginate. This material has potential application as wound healing dressing or face mask.

The increasing popularity of cellulosic materials for 3D biofabrication has been expedited by the commercialization of some printable ink products such as CELLINK from CELLINK AB (Sweden). CELLINK which first was introduced in 2016 is composed of 2% (w/w) CNF produced in aseptic conditions, and sterile sodium alginate at 0.5% (w/w). In a study by Martínez Avila et al.,[74] the ink was mixed with human nasal chondrocytes (hNC) and the produced bioink was bioprinted followed by crosslinking using $CaCl_2$ solution. The bioprinted construct was evaluated for auricular cartilage. The construct showed proper shape and size stability as well as improving the cell viability

Table 2. A summary of recent studies on 3D printing of cellulose-based materials.

Nanocellulose type	Ink composition	Printing method	Cell lines	Bioink	Biomedical applications	Ref.
CNF	CNF/$CaCl_2$ + chitosan oligosaccharides+ poly-l-lysine+protamine	Cell-laden, Inkjet spray	Mouse fibroblasts, human embryonic kidney cells, and human newborn foreskin fibroblasts (Hs68)	Yes	Skin tissue mimics	[122]
CNF	CNF + CMC/alginate	Hydrogel direct ink writing (DIW)	Human primary pancreatic cells	No	Cell culture and disease study	[123]
CNF	CNF/1,4-butanediol diglycidyl ether	Hydrogel DIW	Human fibroblast cells	No	Wound healing	[124]
CNF	CNF-alginate/$CaCl_{2+}$ hyaluronan + H_2O_2	Hydrogel DIW/cell-laden	Mouse mesenchymal stem cell line C3H10T1/2	Yes	3D cell culture of adipocytes	[125]
CNF	CNF-alginate/$CaCl_2$	Cell-laden Hydrogel	Human chondrocyte and mesenchymal stem cells	Yes	Tissue engineering	[126]
CNF	CNF-alginate/$CaCl_2$	Hydrogel DIW	Bovine chondrocyte cells	Yes	Cartilage tissue engineering	[127]
CNF-CNT	CNF-CNT/KOH	Hydrogel DIW	Human neuroblastoma cells	Yes	Neural tissue engineering	[76]
CNF/gelMA	CNF/gelMA + Irgacure 2959	Hydrogel DIW	Mouse fibroblast cells; viability	No	Wound healing	[78]
Enzymatic CNF	CNF + alginate; CNF + hyaluronic acid	Hydrogel DIW	Pluripotent stem cells	Yes	Articular cartilage repair	[128]
CNF/PU	CNF/polyurethane + polyethylene oxide	Hydrogel DIW	Mouse and human fibroblast cells	No	Tissue engineering	[79]
CNF/GGMMAs	CNF/GGMMAsIrgacure 2959	Hydrogel DIW, cell-laden	Human dermal fibroblast and pancreatic tumor cells	No	Tissue engineering	[106]
CNF/TEMPO	CNF + alginate/Ca^{2+}	Hydrogel DIW	L929 mouse fibroblasts	No	Wound dressing devices	[129]
CNF/TEMPO	CNF, TEMPO-CNF, Or acetylated TEMPO-CNF	Hydrogel DIW	Cardiac myoblast cells	Yes	Cellular processes and tissue engineering	[130]
CNF/TEMPO	CNF + gelMA	Hydrogel DIW, cell-laden	NIH 3T3 fibroblast cell-laden	No	Biomedical scaffolds	[131]
CNC	CNC–gelatin conjugates	Hydrogel DIW	Human breast cancer MCF-7 cells	No	Tissue engineering and regenerative medicine	[132]
CNC	CNC + oxidized dextran/gelatin	Hydrogel DIW	3T3, CCK-8, and Hoechst 33342/PI double-staining assays	Yes	Tissue repair	[133]
CNC	CNC + yeast cell + binder (PEGDA) + photo initiator	Viscous paste DIW, cell-laden	Yeast cell-laden	No	Microbial biocatalysts, bioremediation	[134]
CNC	CNC/gelatin+ $CaCl_2$	Hydrogel DIW cell-laden	Mouse fibroblast and human hepatoma cells; viability	Yes	Tissue engineering	[135]
CNC-CNF	CNC/gelatin + $CaCl_2$	Hydrogel DIW	Human nasoseptal chondrocytes	Yes	Cartilage tissue engineering	[136]
Bacterial CN	CNF + silk + gelatin + glycerol	Hydrogel DIW	L929 fibroblasts cells	Yes	Repair of soft tissues	[137]
CM-CNF	CNF + bacterial cellulose (culture medium)	Hydrogel DIW	Fibroblast cells	No	Artificial blood vessels and engineered vascular tissue scaffold	[138]
CM-CNF	Methyltrimethoxysilane hydrophobic CNF matrix-assisted	Hydrogel DIW	A549 lung cancer cells	No	Open cell culture platform and drug test	[139]
M-CMC	M-CMC/LAP	Hydrogel DIW	Fibroblast cell line (NIH/3T3)	No	Biomedical application field	[140]

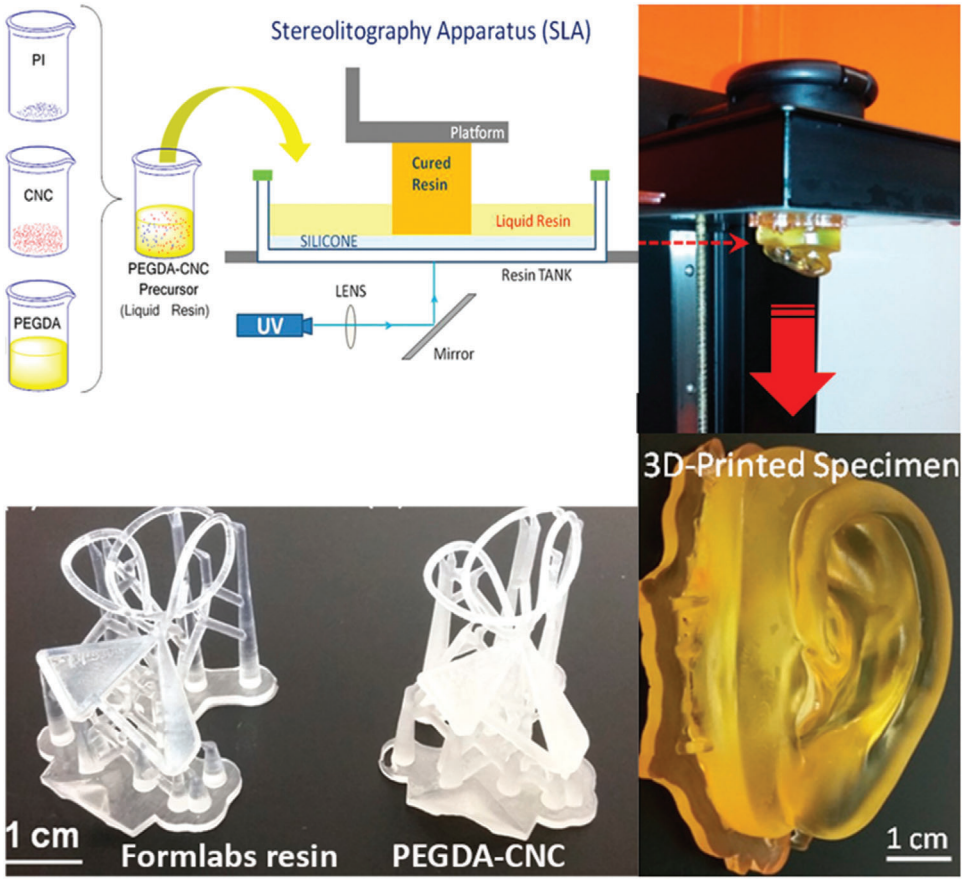

Figure 3. The photocurable liquid resin is composed of the polymer matrix (PEGDA), the nanofiller (CNC), and the photoinitiator (PI) system. Formlabs SLA 3D printing butterfly test specimen using formulated PEGDA-CNC compared to Formlabs resin, and the human ear construct was printed. Reproduced with permission.[75] Copyright 2017. American Chemical Society.

and proliferation. The cells cultured in the 3D structure could express and synthesize GAGs, collagen type II, aggrecan, and matrilin 3, which is an important cartilage-specific ECM protein to maintain the matrix stability and integrity. These promising results could be related to the suitable 3D microenvironment that the CELLINK provides, mimicking the cells' natural matrix. Currently, CELLINK has been modified with tricalcium phosphate, RGD peptides, fibrinogen, and laminins, to be developed into a series of printable inks for various bioprinting applications.

Cellulose nanocrystal (CNC) is another essential cellulosic form which has been assessed as a functional filler for mechanical property improvement. CNC could enhance stiffness, biocompatibility, and hydrophilicity of PEG structures fabricated through mask-based stereolithography.[75] Indeed, CNC has been shown to have a specific modulus comparable to the specific modulus of steel. Palaganas et al. assessed the suitability of CNC for 3D printing while utilizing stereolithography for PEG structure development with improved mechanical properties for biomedical applications.[75] Photocurable resins that have been cured using ultraviolet light were employed in the stereolithography apparatus (SLA) as illustrated in the experimental setup presented in **Figure 3**.

In this study, lithiumphenyl(2,4,6-trimethyl benzoyl)phosphinate (LAP) was employed as a photoinitiator, characterized by excellent photon absorption, water solubility, and biocompatibility. The PEG was further sensitized with the dye, Reactive Orange 16 to improve photon energy adsorption and its transmission into adjacent molecules. However, this overlapped curing system can result in an unwanted increase in the volume of the structure. To address this issue and regulate the effects of radical concentrations, TEMPO oxidation was also introduced. The addition of 0.3 wt% of CNC resulted in a 100% increase in Young's modulus of the hydrogel (from 0.6 ± 0.2 to 1.2 ± 0.3 MPa).[75]

Scaffolds with the ability to support neuron cells are of high importance for neural tissue engineering and brain study applications. In a study by Kuzmenko et al.,[76] cellulose nanofibers (CNF) and carbon nanotubes were formulated into 3D-printed structures with the diameter and electrical conductivity of less than 1 mm and 0.38 S cm^{-1}, respectively, as highlighted in **Figure 4**. The electrical conductivity of the scaffold achieved through the incorporation of carbon nanotubes (CNT) is one of the critical parameters that facilitated cell development and proliferation. The CNF and CNT were mixed at a mass ratio of 4:1. The material was 3D printed through a piezoelectric microvalve and a 300 µm nozzle. Dispersal of CNT in water to enhance its mixing with other materials usually requires the introduction of surfactant molecules to the mixture. However, the introduction of

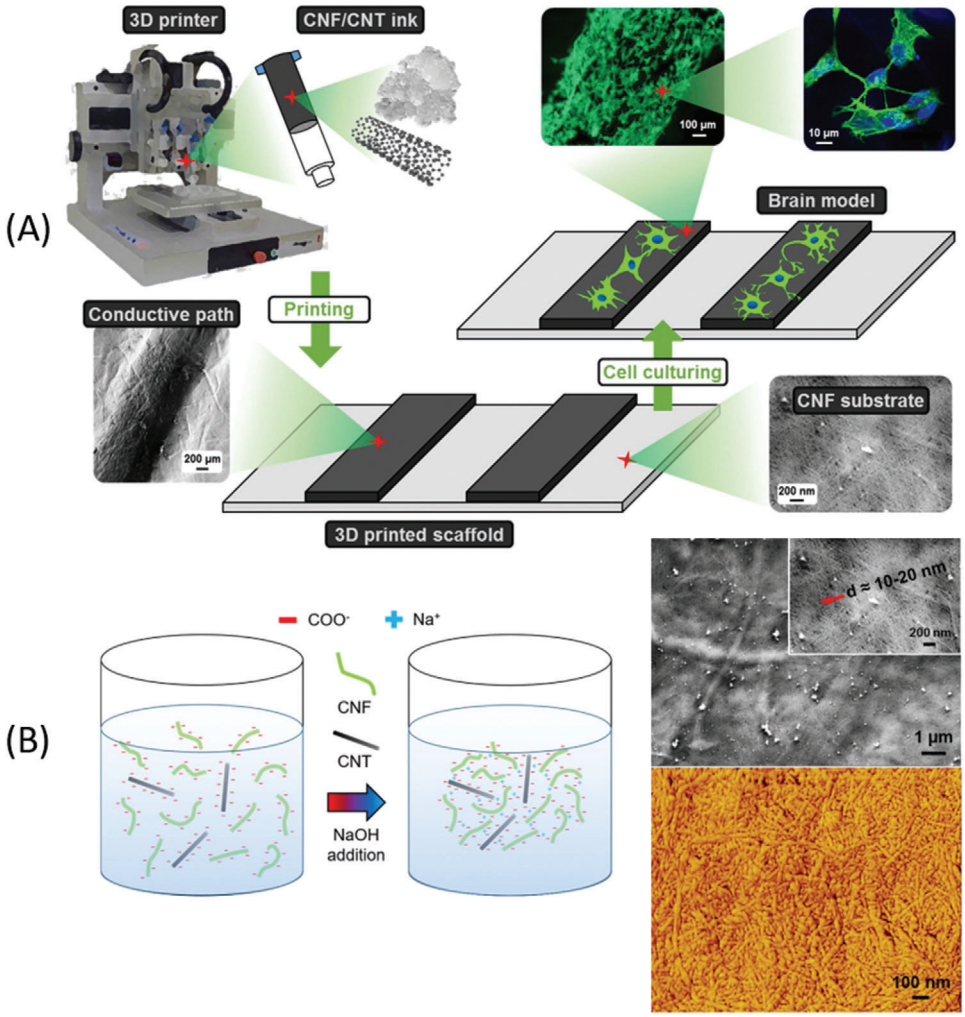

Figure 4. A) Illustration of the development of conductive composite inks through the incorporation of carbon nanotubes into cellulose nanofibrils for 3D printing materials with nanosized surface features and electrical conductivity.[76] B) The addition of NaOH to the ink decreases electrostatic repulsion between colloidal particles while colloidal stability is preserved resulting in ink with rheological properties like the pure CNF. Reproduced with permission.[76] Copyright 2018, Elsevier.

surfactants may result in cytotoxicity toward the cells. Alternatively, CNT may be charged electrostatically to allow for good dispersion of CNT in the mixture through the formation of electro statistically stable structures. Despite an excellent homogeneous dispersion, the resulting ink is not printable due to low viscosity as a result of a high electrostatic repulsion, high negative charge within the ink, and therefore lower entanglement of the fibrils and consequently reduced viscosity of the ink. That being said, the inclusion of sodium hydroxide can moderate the magnitude of electrostatic repulsion forces between colloidal particles (Figure 4).

There is a wide range of studies on the inclusion of lignocellulosic materials into other polymers to mainly improve the structural stability of the structure. Campodoni et al.[77] investigated the effect of cellulose nanofibrils and crosslinking on the mechanical properties of molded gelatin 3D scaffolds, with the primary aim of obtaining good biomimicry and structural stability. The degree of crosslinking was largely affected by the selected method, where it varied from 1.5% for hexamethylenediamine (HMDA) to about 15% when the mixture crosslinked with HMDA, genipin, and a dehydrothermal treatment (DHT). Dehydrothermal treatment includes the formation of covalent bonds between polymer chains without any bridging molecule and is a suitable technique to develop a stable scaffold. The addition of 10% CNF to the gelatin matrix followed by crosslinking with HMDA, DHT is suitable for developing a porous scaffold with tunable mechanical properties. Nevertheless, for the scaffold developed through a solution casting method, there is limited control of the composite resolution and line spacing of the structure, which may affect the final functionality of the scaffold, and this time-consuming crosslinking approach cannot be adopted for 3D printing approach.

Cellulose nanofibrils biocompatibility making it valuable for the development of hydrogels for biomedical applications. Xu et al.[78] developed a 3D printable biomaterial ink using 1% of TEMPO-oxidized CNF with less than 1% of GelMA and reported

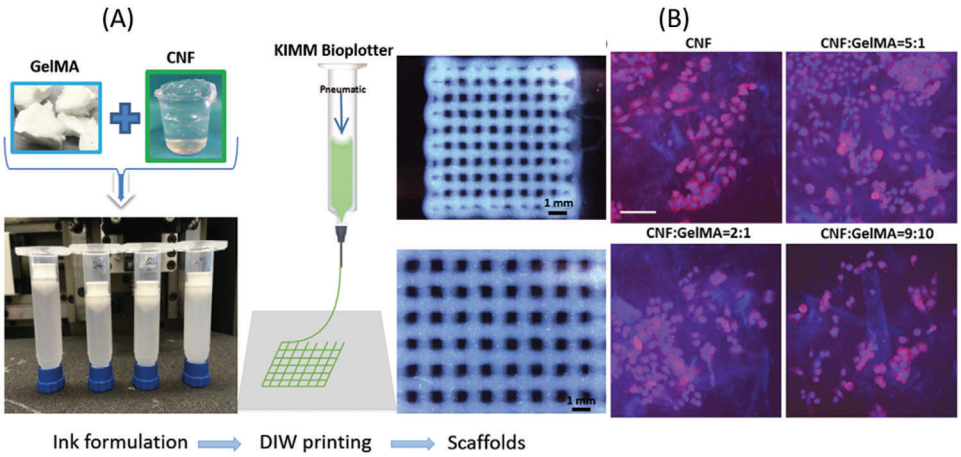

Figure 5. A) Schematic illustration of biomaterial ink formulation and scaffold printing, from left to right: images of GelMA and CNF hydrogel and the process of the formulation; simple drawing of direct ink writing (DIW) process; optical microscopic images of printed hydrogel structures. B) Confocal images of 3T3 cells were seeded onto the scaffold and incubated with the 3D structure on day 3.[78] Reproduced with permission.[78] Copyright 2019, American Chemical Society.

that the UV crosslinking ability of the GelMA was increased in the presence of CNF, as illustrated in **Figure 5**. Although a very low concentration of either CNF or GelMA was used in this study, a structurally stable hydrogel with a mechanical strength of 2.5–5 kPa was obtained which can be due to presence of a strong physical interaction between CNF and GelMA, as a result of strong hydrogen bonding and physical entanglement. GelMA may also be adsorbed on the CNF layers. The gelatin methacrylation possibly influences the interaction of the CNF and gelatin as a result of the steric effect of grafted methacryloyl groups and their hydrophobic nature. Interestingly, the addition of GelMA into the CNF hydrogel has improved the cell compatibility of the structure and improved the proliferation of adhered fibroblasts. This formulation has great potential for developing 3D structures for wound healing applications.[78]

In addition to the inclusion of CNF to the gelatin matrix to improve the mechanical properties, CNF has also included in the polyurethane (PU) mixture to improve its printability.[79] Where CNFs could link PU nanoparticles in the structure resulting in a printable paste with pattern fidelity and stability (**Figure 6**). New urethane bonding was formed between –OH groups of CNF and the isocyanate which resulted in an improved crosslink density of CNF-PU samples compared to the control PU. The web-like structure of CNF also played a role as a filler to improve the mechanical properties of the paste.[80]

PU/CNF composites can be prepared either through the dispersion of the CNF in the PU, or by its inclusion during in situ syntheses of the PU. The carboxyl group content of CNF plays a vital role in the viscosity of the matrix; this can be explained by the presence of repulsion force between PU nanoparticles with abundant COO– on their outer surface. This is also the case for CNFs with hydroxyl groups. These two negatively charged groups of COO– on PU and CNF repel each other and limit the interaction of PU and CNF. The higher the carboxyl group content, the more potent repulsion force and harder interaction, therefore, a charge neutralizer such as triethylamine (TEA) is required. For the in situ synthesis of PU/CNF composite, a 3% suspension of CNF was added during the synthesis of PU in the presence of TEA. Sonication mixing after PU synthesis was used as a simple method for dispersion of CNF in the mixture, although the mixture did not have suitable viscosity for printing. To adjust the viscosity, the addition of extra TEA right after CNF dispersion was needed; otherwise, the PU particles become stable after formation and interactions between CNFs and PU particles are no longer possible.

TEM images indicated to the formation of a skewer like structure between cellulose fiber and PU, justifying how CNF affects the viscosity of the PU.[79]

Combining directional freeze casting and 3D printing, Kam et al. developed a method called direct cryowriting (DCW). Using this technique, rod-shaped nanoparticles of cellulose nanocrystals and xyloglucan (XG) were aligned through freeze casting of the solution which was then printed at cryogenic temperature using an extrusion-based 3D printer. The growth of ice crystals in this technique controls and guides the alignment of the particles. The presence of XG at a low concentration (<4%) can act as a crosslinking agent in adhering to the cellulose nanoparticles together in the 3D-printed structure and enhancing the viscosity of the mixture, thus making it printable. Nevertheless, XG at high concentrations can cover the surface of the particles and negatively affect the rheology of the mixture by making the particle surface slippery. This technique may develop into 3D printing of objects with controlled morphologies and mechanical properties, as shown in **Figure 7**I.[81]

Another approach for the development of a cellulose-based biomaterial was demonstrated by Lewis et al.[82] and illustrated in Figure 7II. In their work, cellulose nanocrystal physical gels were prepared through freeze-thaw cycles of the CNC suspensions. In this novel approach, the negatively charged sulfate half ester groups existing on the surface of the CNC provide electrostatic repulsion force which stabilizes the particles in the suspension, while the growing ice crystals induce irreversible aggregation of CNC upon freezing. The confinement of CNC during freezing also leads to the domination of the van der Waals forces, resulting in the aggregation of the CNCs into cluster sheets preventing its redispersion upon thawing. Thus, after each freeze-thawing

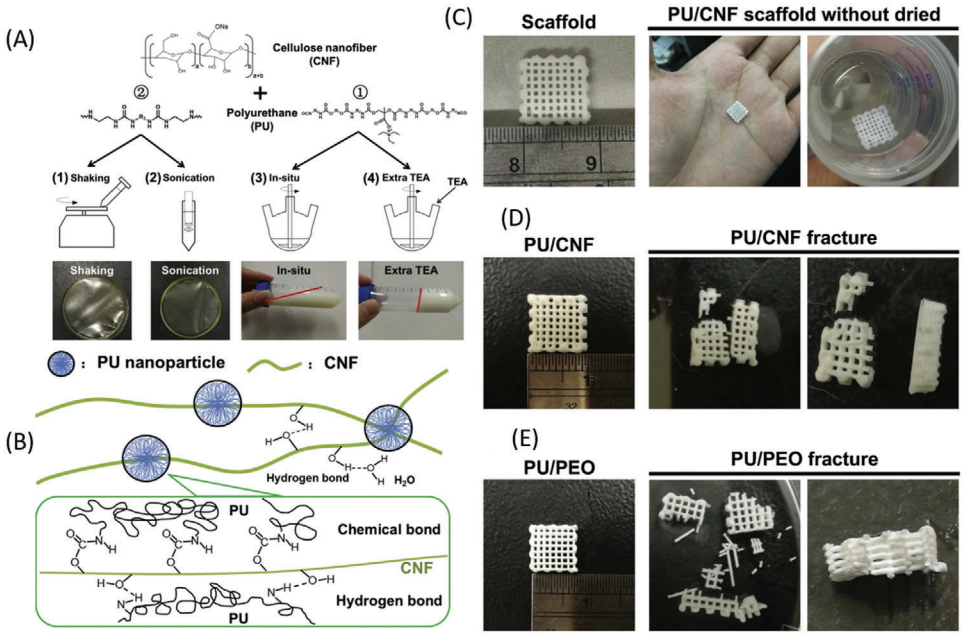

Figure 6. A) Preparation of polyurethane (PU)/cellulose nanofibrils (CNF) nanocomposites using different techniques of shaking, sonication, in situ synthesis, and in situ with the addition of extra charge neutralizer triethylamine (TEA). B) Illustration of the molecular interaction of PU and CNF during the formation of the nanocomposites. C–E) Images of the printed scaffolds of PU/CNF and PU/PEO.[79] Reproduced with permission.[79] Copyright 2019, Elsevier.

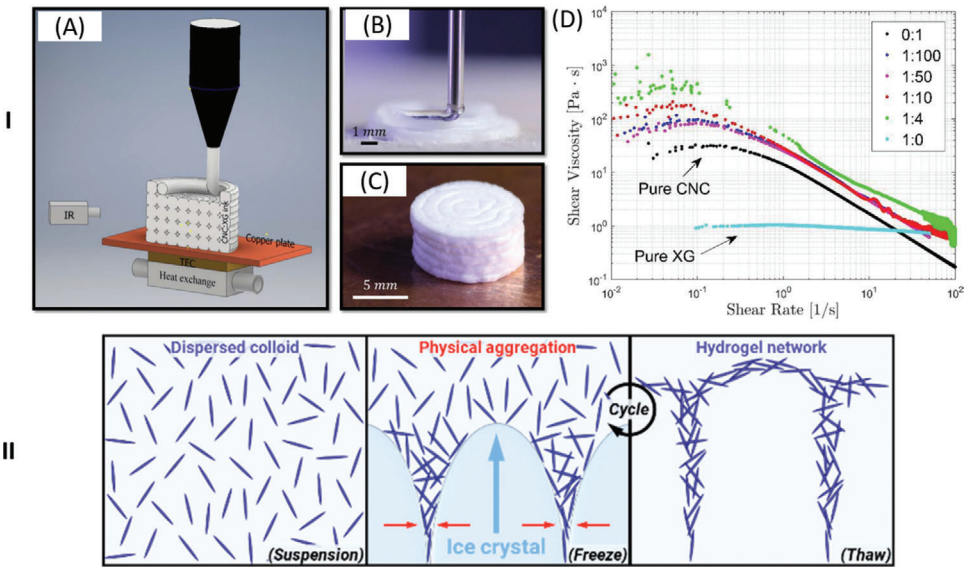

Figure 7. I) Schematic illustration of the direct cryowriting (DCW) setup A), image of the DCW printing process B), final scaffold C), and viscosity measurements of mixtures of XG and CNCs at different ratios indicates the influence of XG content on the viscosity and the shear-thinning behavior of CNCs D). Reproduced with permission under the terms of the Creative Commons License.[81] Copyright 2019, the Authors. Published by MDPI. II) Freeze-thaw gelation caused by a physically confined aggregation of CNCs between growing ice crystals. The CNCs do not fully redisperse when thawed.[82] Reproduced with permission.[82] Copyright 2019, American Chemical Society.

(FT) cycle CNC aggregates into larger clusters. This physical colloidal gel can be used for the formation of 3D hydrogel networks with diverse biomedical applications. This technique is simple, requires low concentrations of the CNC (4%), is free from chemical additives such as salt and it is possible to tune the rheological properties of the hydrogel by changing the parameters such as freezing temperature and cooling rate, number of FT cycles and concentrations.[82]

In another study, the effect of CNF and bioactive glasses on the rheological properties of alginate/gelatin bioink was inves-

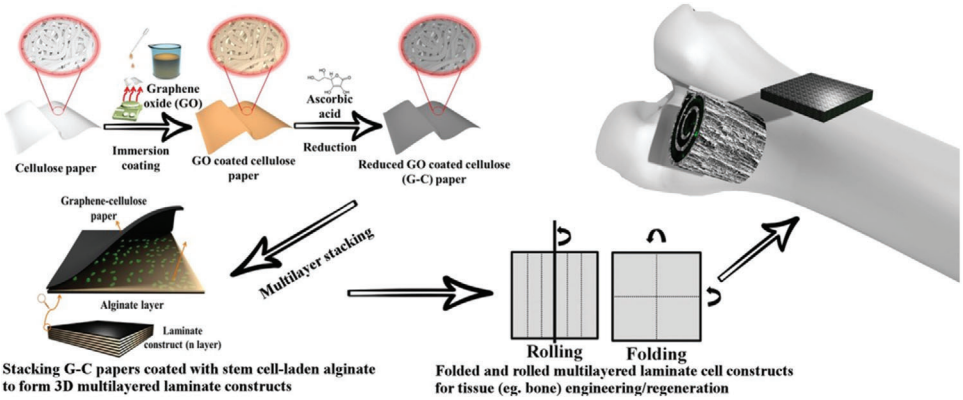

Figure 8. Assembly of the graphene–cellulose paper. Folded and rolled multilayered cylindrical laminate constructs depicting cells embedded in alginate between layers.[84b] Reproduced with permission.[84b] Copyright 2018, Elsevier.

tigated, and the response of bone cells embedded in this matrix was evaluated.[83] By modulating the flow behavior of the hydrogel, CNF enhanced the printability of the material. Bioactive glasses introduced bioactive cues of bone cells and induced the differentiation of the cells; nevertheless, the addition of this ceramic phase could result in increased viscosity and negative effect on the printability of the scaffold as a result of phase separation between the solution and ceramic phase. Therefore, CNF was also introduced to enhance the rheological properties of the material. Knowing that gelatin and CNF have hydroxyl groups on the surface and gelatin has amine and carbonyl groups, gelatin and CNF can interact via the formation of hydrogen bonds. In the case of a TEMPO-oxidized CNF, this would also have aldehyde groups on the surface which can interact with the amine groups of the gelatin through a Schiff base reaction which explains the effect of CNF on enhancing the viscosity of the material.[83]

Cellulose paper coated with graphene was evaluated for potential application as a 2D or 3D support of human cells.[84] The material is produced by immersion deposition first with graphene oxide which is then converted to the reduced form (RGO). The proliferation and osteogenic differentiation of adipose-derived stem cells indicated the suitability of the developed graphene cellulose paper material for fabricating 3D multilayered laminate cell-laden bone constructs. Using this simple immersion technique does not require specific materials or equipment and result in a uniform distribution of RGO on the cellulose substrate. In addition, lamination of this paper with alginate hydrogel followed by its folding into origami cuboid or cylindrical structure make 3D cell support structures from this material. This technique is a combination of the mechanical properties from commercial cellulose paper and the microscale morphological properties of RGO, resulting in a material that helps adhesion of human cells growth and differentiation (**Figure 8**).[84b]

3.2. Methylcellulose

Methylcellulose has been used as a supportive biomaterial for biofabrication in various ways, such as sacrificial ink and stabilizing components, particularly for extrusion based bioprinting. Knowing that ink viscosity of plays an important role in printability, methyl cellulose has been largely used to adjust the viscosity of the ink. MC is characterized by a viscosity ranging from 5 to 75 000 cP in 2 wt% solution.[38] In different studies MC with both low (15 cP) and high viscosity (4000 cP) have been used for bioprinting although it was not possible to develop multiple stacked layers using the low viscosity MC.[34,85] Although MC can form a viscous hydrogel network, its poor mechanical properties limits its application for bioprinting in unmodified form. To address this issue, Shin et al.[86] in a recent study developed a dual cross linkable tyramine-modified MC conjugate which could be printed and showed good mechanical properties. In this study, reversible thermal cross linking was combined with photo crosslinking to form the hydrogel (**Figure 9**). First, carboxylic acid groups were introduced in the backbone of MC, to then be coupled to tyramine. The hydrogel was covalently cross linked in the presence of photosensitive derivatives of vitamin B2 used as a photo initiator.

Methylcellulose has also been used in combination with alginate for bioprinting. In a recent study, an alginate–MC blend was used for encapsulation of human chondrocytes or human mesenchymal stromal cells, and printed with a calcium phosphate paste (CPC) as an osteochondral tissue substitute. Using alginate/MC with CPC a stable zonal structure was printed that supported the cells' viability.[87] In addition to alginate, hyaluronic acid has also been blended with MC for bioprinting, and it was observed that the addition of HA to the mixture decreased the sol–gel transition temperature, as well as slowed the gelation process. While different studies exist on 3D bioprinting of MC individually[31] or in combination with other polymers, a systematic comparison to reveal the real advantage of preparing these blends is lacking. The readers are referred to the mini review paper by Ahlfed et al.[34] which highlighted various applications of MC for biofabrication.

3.3. Microbial Cellulose

The rheological and mechanical properties of MBC make it a suitable substitute for the natural extracellular matrix (ECM). The viscous and elastic properties of MBC hydrogels affect cell be-

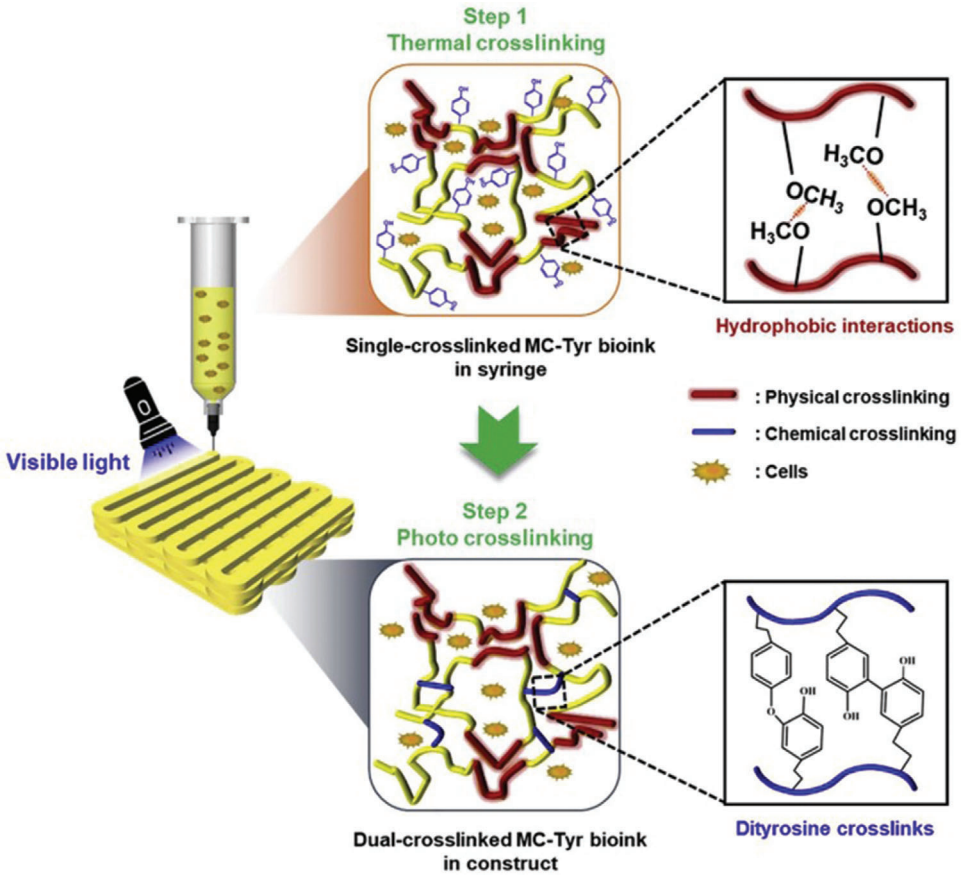

Figure 9. Schematic of the 3D bioprinting process via the dual crosslinking system (thermal and photo-cross linking) of Methylcellulose–Tyramine bioink.[86] Reproduced with permission.[86] Copyright 2020, Elsevier.

havior in terms of proliferation and spreading.[88] Biocompatibility and moldability of MBC hydrogels have been used to develop 3D structures which have been suggested suitable as an implant for cuff for nerve suturing, artificial blood vessel, and scaffold for regenerative medicines.[89]

An ideal wound dressing should have easy and painless removal, facilitate the healing process, be nontoxic, provide wound infection protection, and mimicking the natural extracellular matrix.

That being said, MBC has been widely studied in the literature as the wound dressing material.[90] Various materials (biopolymers, organics, inorganics, etc.) are incorporated into MBC such as silk sericin,[91] graphene oxide reinforced chitosan,[92] silver sulfadiazine loaded MBC/sodium alginate,[93] hyaluronan/MBC nanocomposites,[94] copper oxide/MBC,[95] ampicillin/gelatin-MBC,[96] and human urine-derived stem cells loaded/MBC.[97] Stiffness and low strength under hydrophilic conditions limit MBC for biomaterial applications as commercial products, and fabrication should be followed by other treatments such as plasma treatment, reducing agents, ex situ method, shaking at low speed, and freeze-drying.[57]

Bacteria produce cellulose usually at air–water interfaces, a process that suffers from the absence of a 3D macroporous structure. This lack of having a porous structure limits MBC application for developing biomaterials as the cells cannot penetrate, proliferate, and eventually regenerate the tissue. To address this issue, a foamed MBC with defined porosity was created through a direct foaming technique.[98] By saturating the bacteria's oxygen dependency, the cellulose was grown by the air bubbles and stabilized using Cremodan (Danisco) as a biocompatible surfactant and xanthan gum as a green thickener to stabilize the foam. Considering viscosity as an important parameter affecting the formation of the cellulose, the authors fine-tuned and controlled the formation of MBC by changing the concentration of the thickening agent. With this relatively straightforward technique, a 3D-foamed biofilm was produced with potential for biomedical applications (**Figure 10**I).[98] Strong nanofibrils and high-water retention capacity of MBC make it attractive for 3D printing; however, the disentanglement of intricated MBC fibrillar networks is one major challenge toward 3D printing of MBC for biomaterial applications which if not correctly disentangled can block the printer nozzles. Using the aqueous counter collision technique which is based on collision energy of dual water jets, Apelgren et al.[99] disintegrated bacterial cellulose nanocrystals into fibrils. The biomaterial ink developed based on the aqueous counter collision (ACC) treated MBC showed excellent printability with structural integrity and postprint stability (Figure 10II). The authors indicated ACC treatment as a suitable method to develop printable materials from bacterial cellulose which could support the proliferation and growth of chondrocytes.

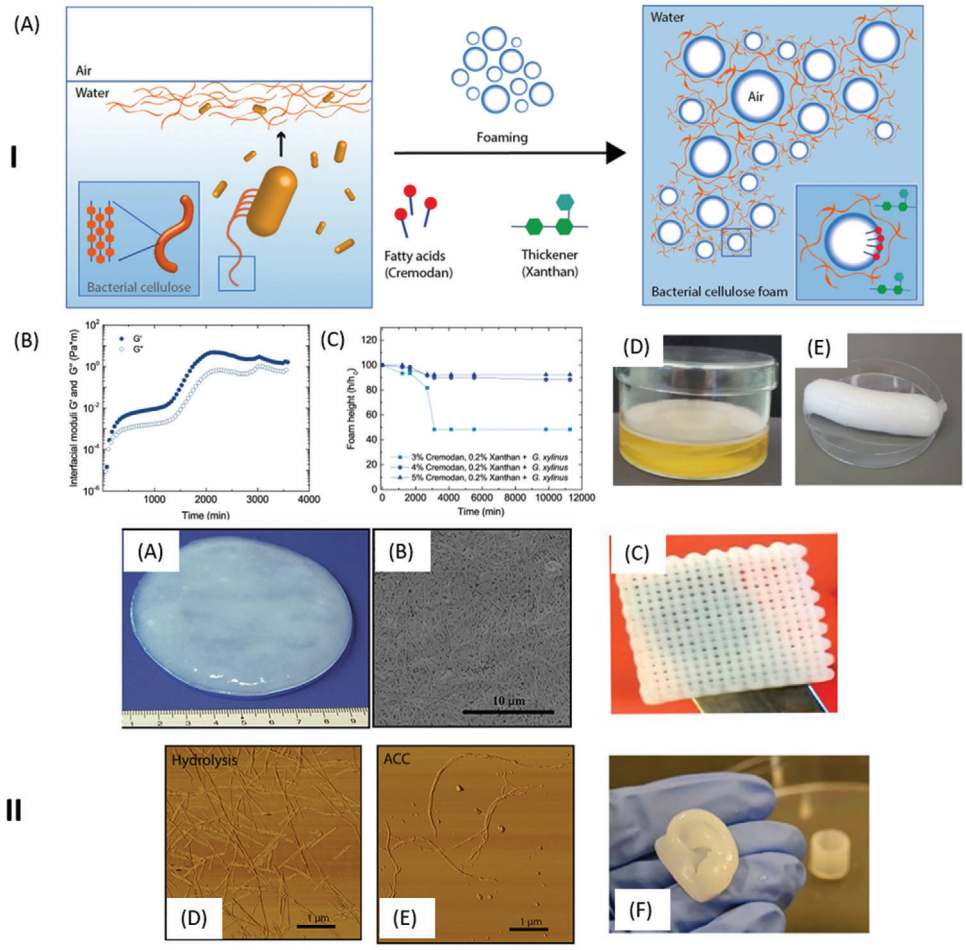

Figure 10. I). The bacterial cellulose developed as foam after 7 days of bacteria inoculation using 3 wt% Cremodan as surfactant and 0.5 wt% xanthan as the thickening agent. Reproduced with permission under the terms of the Creative Commons License.[98] Copyright 2018, the Authors. Published by Springer Nature. II) The BNC fibrils with a complex 3D structure were well dissembled using both hydrolysis and the aqueous counter collision (ACC) method with average fiber diameter of 16 ± 0.07 nm and 2 ± 0.4 µm length. Structures bioprinted with high resolution and stability using bacterial cellulose after disassembly.[99] Reproduced with permission.[99] Copyright 2019, American Chemical Society.

In another study,[100] MBC was sonicated to facilitate its fragmentation and subsequently blended with a 10% PCL solution before it was 3D printed into scaffolds with 100 µm line spacing using an electrohydrodynamic printer. Fibroblast cell lines were subsequently seeded on the printed scaffold to evaluate the biocompatibility of the developed structures. The study showed that when compared to pure PCL scaffolds, the MBC/PCL scaffolds showed better cell viability.

Edible solid foams with a 3D porous structure have attracted attention due to biodegradability and excellent biocompatibility in various applications, e.g., functional food products, drug delivery systems, nutrients, etc.[101] Foams were generally produced using surfactants or polymeric matrix in order to self-assemble to liquid/liquid or air/liquid interfaces to form lightweight, highly porous foam structures. However, many types of foam were too unstable and brittle for utilizing in multi-functional applications. To enhance the mechanical strength of foams, adding polysaccharide particles with high specific surface area, e.g., starch, cellulose, and chitin has been suggested.[102] Pickering emulsion technology using particle-stabilizer contents was proposed as a new strategy to adjust the pore diameter, porosity, and mechanical properties of foams. Zhang et al. investigated edible foam (MBC/soy protein) based on Pickering emulsion templating. The edible solid foams with excellent mechanical property were fabricated via aggregation of nanoscale soy protein and adsorption on MBC nanofibrillar networks with porous structures, showing good energy absorption capacity, and noncytotoxicity to cells. MBC, as a promising Pickering stabilizer can adsorb at oil/water interfaces. The volume ratio of oil/water influences the microstructure and rheological properties. It was noteworthy that a slight decrease occurs in the plateau stress with increasing oil volume due to the denser pore structure (**Figure 11**).[103]

Improving the dressing properties of BC such as water retention facilitates its application for medical usages. Alginate as a green hydrophilic component was used to increase the water retention properties of BC to obtain a smooth dressing for wound application. The fabrication process of BC/alginate composites is shown in **Figure 12**. The modification process did not affect the desired properties of the original BC, e.g., biocompatibility and mechanical stability. The fabricated dressings were impregnated

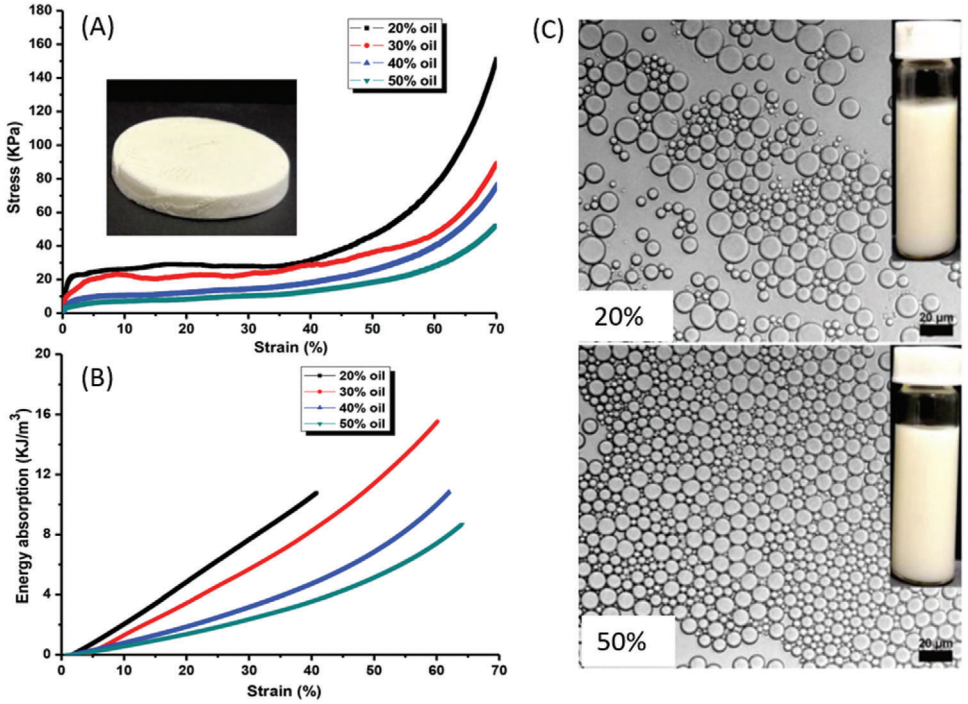

Figure 11. Edible solid foams: A) compressive stress–strain curves, B) the energy absorbed–strain curves (SPI concentration 3.0 wt%, and the ratio of optical micrographs of emulsions complexes soy protein isolate/TEMPO-oxidized bacterial cellulose (SPI/TOBC) 12.5:1 (w/w)), and C) SPI/TOBC complexes with oil fraction 20% and 50% at pH 7.[103] Reproduced with permission.[103] Copyright 2020, Elsevier.

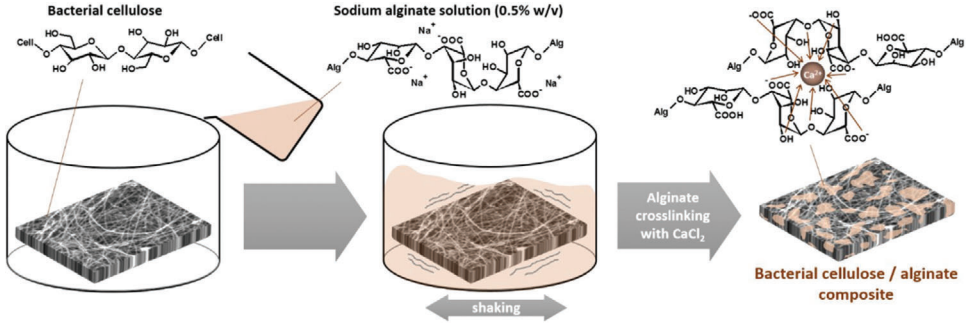

Figure 12. The fabrication process of BC/alginate composites as a skin wound dressing releasing antimicrobial polyhexamethylene biguanide (PHMB).[104] Reproduced with permission.[104] Copyright 2020, Elsevier.

with antimicrobial poly (hexamethylene biguanide) hydrochloride (PHMB). The as-prepared wound dressing demonstrated a good release rate and an attractive approach for large-scale fabrication.[104]

3.4. Hemicellulose

Hemicellulose with free hydroxyl groups can be subjected to a range of functionalization including etherification and esterification. Liu et al.[105] introduced different hemicellulose, e.g., xyloglucan (XG), xylan, and galactoglucomannan into the nanofibrillated cellulose through in situ adsorption and pre sorption to modify the structural and mechanical properties of the cellulose hydrogels for wound healing applications. Incorporation of 10% XG was reported as the most beneficial in supporting the growth and proliferation of the fibroblast cells (NIH 3T3). While the research generated interesting results, the versatility of the hydrogels when subjected to higher conditions of temperature and pH conditions may be of interest in future studies as higher pH values typically characterize infected wounds. The multifunctionality of the hydrogels may also be explored.

Being inspired by the affinity of heteropolysaccharides to cellulose, Xu et al.[106] developed a range of UV crosslinkable galactoglucomannan methacrylates (GGMMAs) with different degrees of substitution resulting in materials with tunable rheology and mechanical properties (2.5–22.5 kPa). The synthesized ink showed fast gelation properties suitable for extrusion-based 3D printing. In addition, derivatives of hemicellulose such as tyramine modified, thiol functionalized, or methacrylated hemicellulose have been investigated as promoting agents for the develop-

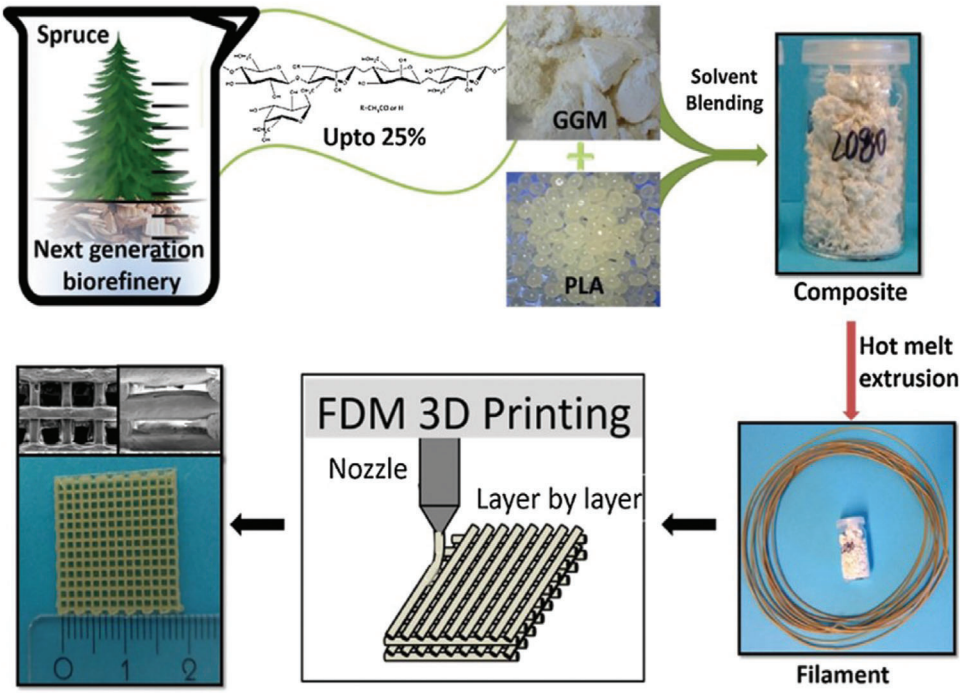

Figure 13. Schematic illustration of the preparation of composite of galactoglucomannan (GGM) and PLA, filaments, and scaffolds by FDM 3D printing. An example of a composite ratio of 20:80 in weight of GGM and PLA is shown.[113] Reproduced with permission.[113] Copyright 2018, Elsevier.

ment of 3D-printed nanocellulose inks. In another study, Markstedt et al.[107] developed an all wood-based ink for 3D printing via crosslinking of the cellulose nanofiber using modified tyramine functionalized xylan. This tyramine modification made xylan crosslinkable and the authors could develop a range of inks with various rheological properties depending on the degree of xylan modification and the ratio of the modified xylan to the cellulose.

The previous investigation showed that the combination of cellulose nanocrystals (CNCs) and xyloglucan (XG) has the potential to yield composites that mimic the plant cell wall.[108,109] The freeze-casting of aqueous inks composed of a mixture of CNCs and XG was presented by Kam et al.[81] The hydrogen bonding and van der Waals forces drive the binding of XG to cellulose surfaces and their crosslinking leads to an extensible structure.[110] The XG acted as a binder, resulting in an improvement of mechanical properties and induction of internal structure modifications to the 3D-printed construction. However, due to the high concentration of XG the gel structure may collapse.[81] Recently, modified microfibrillated cellulose (MFC) gained attention to produce porous materials due to its high strength-to-weight ratio. The ultrahigh porosity of materials was obtained by adsorption of xyloglucan onto MFC.[111] The MFC/XG foams were fabricated by the adsorption of xyloglucan onto the MFC, followed by degassing and freeze-drying of the suspension. The mechanical properties at different foam densities have been investigated. The cellulose–XG nanocomposite foam was thermally stable up to the degradation point of cellulose (275 °C). In a further study by Josset et al., the modified MFC foam was obtained by a straight forward freeze-thawing–drying procedure.[112] The procedure was involved in the ice-templating step of the MFC/urea suspensions, dewatering of the stabilized porous MFC structures, and, finally, drying of the MFC foam. Galactoglucomannan (GGM) as a major hemicellulose type in softwoods was used to partially replace the synthetic polylactic acid (PLA) in 3D printing constructs (**Figure 13**).[113] The hot–melt extrusion (HME) was applied for the binary biocomposite of GGM and PLA at different ratios. The mechanical property of the composites could be fulfilled in crystallized PLA by replacing up to 20% amorphous GGM.

Recently, Köhnke et al. presented a new method to prepare xylan-based hydrogels from modified hemicelluloses.[114] The procedure used freeze-casting along with a crosslinking process and can be described as a three step by oxidizing xylan with sodium periodate followed by mixing with cellulose nanocrystals (CNCs) and finally crosslinking the hydrogels by unidirectional solidification. The unidirectional solidification resulted in ice-segregation-induced self-assembly and led to concentrated oxidized xylan polymers. Hemiacetal crosslinking bonds were formed between the aldehyde groups and hydroxyl groups during the freeze-casting process. The low-density xylan biofoams with a lamellar structure designed by unidirectional solidification are shown in **Figure 14**.

3.5. Lignin

Some previous studies have involved investigations into the utilization of lignin-containing arabinoxylan (AX) and cellulose nanofibers (CNF) in the preparation of 3D aerogels and hydrogels.[115] In work presented by Berglund et al.,[115] different concentrations of citric acid (CA) were employed in crosslinking, thus promoting swelling of the hydrogels and an improve-

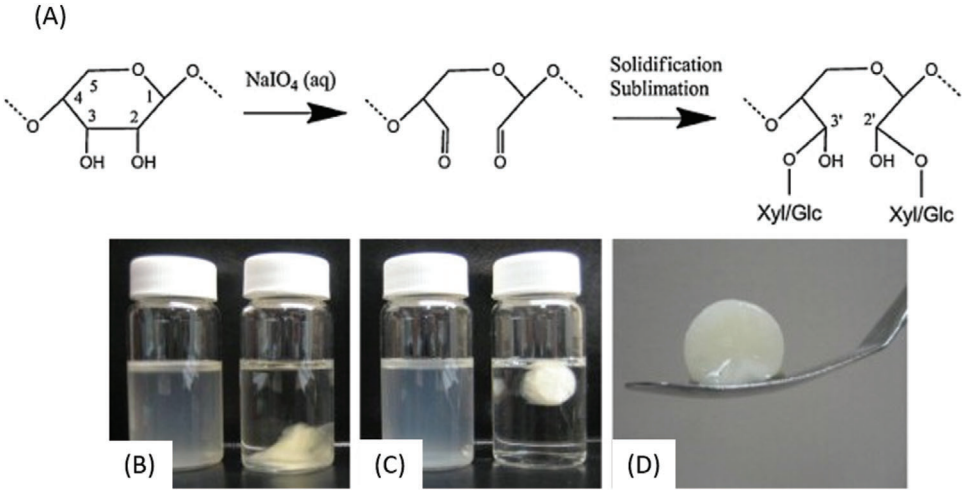

Figure 14. Proposed reactions involved in crosslinking of xylan–cellulose nanocrystal composite hydrogels during freeze-casting.[114] Reproduced with permission.[114] Copyright 2014, Elsevier.

ment in the compressive strength and modulus. Such improvements in the compressive strength and modulus were, however, shown to be accompanied by the deterioration in adsorption performance. The study, therefore, highlighted the need to undertake optimization experiments to determine the optimal concentration of CA that will not lead to a significant deterioration in adsorption performance. The research undertaken by Berglund et al.[115] is particularly important since the aerogel products were shown to be highly porous, lightweight structures which together with the AX-CNF hydrogels were capable of attaining high compressive strength, considered desirable in the field of soft tissue engineering.

The combination of PVA as a matrix template, lignin and a crosslinker (epichlorohydrin) forms superabsorbent hydrogels with a high swelling ratio. The lignin content significantly affects the swelling ratio and strength mechanical of the hydrogel. A mechanism for lignin–PVA hydrogel was proposed as shown in **Figure 15**. The interaction between the epoxy group of the crosslinker and the hydroxyl group of lignin/ PVA leads to ether bond formation. A new epoxy group formed when HCl was removed from the other end of the crosslinker and continued to convert the excess crosslinker to glycerol while hydrogen bonds were formed between hydroxyl groups of lignin and PVA.[116]

Inclusion of carbon nanotubes (CNTs) in lignin-based materials was reported beneficial to increase the mechanical properties of lignin-based nanofibers.[117] 3D fibrous structures were generated via the electrospinning method into diverse structures. The electrospinning composite lignin/CNT/PVA demonstrated a substantial enhancement in terms of breaking stress, modulus, and antimicrobial activity compared to lignin/PVA nanofibers. The dispersion of CNT into polymer matrix depends on functionalization methods, where, e.g., noncovalent CNT functionalization is more effective than the covalent method.[118] The composite lignin and chitosan-based biomaterials are significantly employed as wound dressing materials and pharmaceutics. The lignin-derived from *Artocarpus heterophyllus* fruit peel (anionic polymer). The hydrogen bonding between the –OH, =CO, and R–O–R groups of both lignin, as well as chitosan, exhibits the formation of intermolecular interaction.[119]

The incorporation of lignin into chitosan–PVA composite hydrogel enhances the mechanical strength and the adsorption capacity of the protein. The lignin–chitosan–PVA composite hydrogel (LCPH) effectively improved wound healing in a rat wound model, indicating high potential in skin wound care. The crosslinking mechanism of lignin–chitosan–PVA hydrogels, tensile mechanism and in vivo wound healing activities of LCPHs are shown in **Figure 16**.[120] The ionic bonds were generated between sulfonate groups of lignin and amino groups of chitosan, leading to increasing the hydrogel mechanical strength. The good bactericidal and antioxidant activity along with large tensile deformation and high mechanical strength was observed from the LCPHs. The mouse models result showed that the LCPH provides a moist healing environment and accelerates healing.

The presence of silver nanoparticles shows a promising potential to employ antimicrobial fabrics and wound dressing material.[121] Loading silver nanoparticles over lignin/poly(vinyl alcohol) nanofiber mats via the electrospinning technique indicate growth inhibition zone against *Bacillus circulans* and *Escherichia coli*. Fused filament fabrication (FFF) for is a 3D printing method based on the heating a polymer filament, extruding through a small nozzle and finally solidifying on a build plate. Low coefficient of thermal expansion and high mechanical strength are considered as the most important properties for FFF because of its processability for extrusion applications. Composites comprised of lignin and poly(lactic acid) (PLA) can be prepared using a casting method. However, to employ solvents could provide toxicity issues for healthcare applicants. The combination of lignin and PLA was considered as a composite for FFF applications and introducing curcumin as the model drug. Different meshes were fabricated by 3D printing using composite PLA/lignin in which the first layer contained a PLA/lignin mesh and the second layer was printed using PVA, followed by casting a solution containing a drug. The PVA film contributes to providing a moist environment to the wound and slow release of drugs. When soluble patches containing drugs are layered over

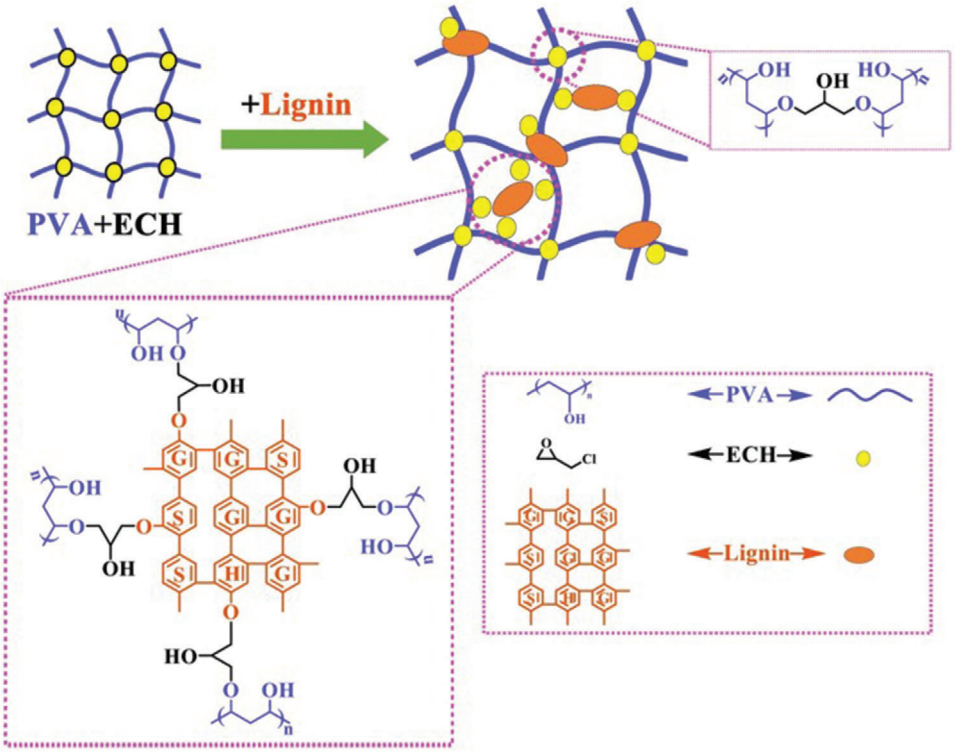

Figure 15. The structure of the lignin–PVA hydrogel.[116] The epoxy groups of the crosslinker, epichlorohydrin, react with the PVA or lignin hydroxyl groups. Reproduced with permission.[116] Copyright 2019, Elsevier.

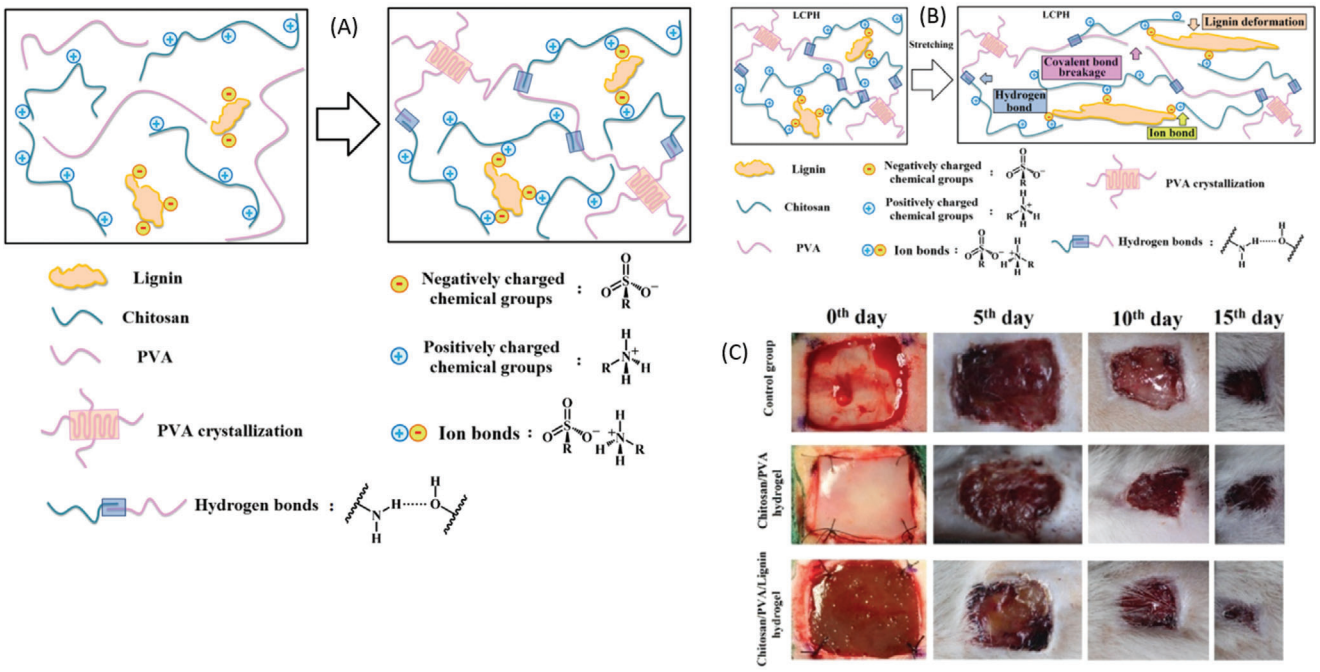

Figure 16. A) The crosslinking mechanism of lignin–chitosan–PVA hydrogels, B) the tensile mechanism of LCPHs, and C) images of wounds with the control group with no dressing, lignin-free dressing, and lignin-containing dressing on the 0th, 5th, 10th, and 15th day after administration.[119] Reproduced with permission.[119] Copyright 2019, Elsevier.

the mesh surface, the drugs can diffuse easily through the mesh pores to the wound as the patch dissolves.

4. Considerations for Using Wood-Based Biomaterials for Biomedical Applications

4.1. Biocompatibility and Toxicity

Biocompatibility is an essential requirement for biomaterials, which should be in harmony with the surrounding tissue.[141] Several studies have evaluated the biocompatibility of cellulosic materials both in vitro and in vivo using various cell lines, methodologies, and techniques.[142] In general, cellulose has been broadly reported biocompatible which in some cases caused low or moderate responses in vivo.[142] Cellulolytic enzymes which are responsible for the degradation of cellulose are not present in the human body; this lack of degradation of cellulose may cause some level of incompatibility. Studies regarding the biocompatibility of cellulosic materials such as CNC and CNF are scarce, and many studies have assumed the materials safe and biocompatible. In some studies, related to cellulosic based hydrogels, the materials were exposed to different cell lines and parameters such as cell viability and proliferation have been evaluated to measure the biocompatibility of the material.[19]

Yanamela et al.[143] studied the pulmonary toxicity of different forms of CNC (CNCS: 10 wt%; gel/suspension and CNCP:powder) by exposing mice to the CNC materials at three different doses (50, 100, and 200 µg per mice) for one time and the results were compared to responses induced by a single dose of asbestos (50 µg per mouse). The tested CNC materials if inhaled showed a dose-dependent damage to the tissue, oxidative stress, and strong inflammatory reactions in the lungs. The observed markers of oxidative stress and inflammatory mediators were more prominent in case of CNCS. The responses caused by CNC were more serious in compared to asbestos. Catalán et al. in another study, administered NFC by pharyngeal aspiration to mice which resulted in DNA damage in the lungs and acute inflammatory response. However, the authors could not conclude if the observed responses were persistent over a long time or were transient.[144] Porous scaffolds prepared from CNF by TEMPO oxidation and carboxymethylation showed no in vitro or in vivo toxicity, but showed biocompatibility with potential reparative applications such as wound healing. Nevertheless, both of the CNF materials when implanted in the animals showed a lack of degradation, which caused well-developed foreign body reaction regulated by secretion of various cytokines.[145] Therefore, the slow or lack of degradation of these materials can impact their potential regenerative applications.

TEMPO-oxidized cellulose materials were particularly found blood compatible with positive biological activities when administered orally for the regulation of postprandial blood metabolic variables such as postprandial blood glucose, plasma insulin, and concentrations of triglyceride. The authors suggested that the TEMPO-oxidized cellulose may act like dietary fibers, which can go through the small intestine without being hydrolyzed, and regulate the metabolic pathways in the postprandial state.[146] Bacterial cellulose is normally considered as a material with better biocompatibility in comparison to other cellulose types which can be due to its different synthesis process. Helenius et al. evaluated the in vivo biocompatibility of BC by implanting it in rats for up to 12 weeks. The implants were evaluated for chronic inflammation, cell ingrowth, angiogenesis, and foreign body responses. No microscopic sign of inflammation was observed and there was no sign of the presence of fibrotic capsule or giant cells formation. Fibroblast cells could infiltrate into the BC implants and the BC implant can be integrated into the tissue.[147] Bacterial cellulose has been used for diverse biomedical applications and has generally been reported safe and nontoxic; the readers are referred to the review paper by Torres et al.,[148] who provided an extensive review of the biocompatibility of the BC that have been used for biomaterials engineering.

Nevertheless, it is important to highlight that despite cells can grow and proliferate in the presence of BC, the surface properties of unmodified BC do not favor cell attachment. Although cellulosic materials have generally been considered nontoxic when studied for oral or dermal toxicity, given the diversity of materials sources, physiochemical properties, type of materials and diversity of chemical modifications that have been applied, the safety of these materials require further, rigorous investigation. Further information concerning the pulmonary, oral, dermal toxicity and cytotoxicity of cellulose nanocrystals have previously summarized in a review by Roman.[149]

4.2. Degradation

The stability and degradation rate of polymeric biomaterials is an essential parameter in biomaterials engineering. Cellulose in nature is a mixture of crystalline and amorphous regions. The amorphous fractions reduce the stiffness of the material while depending on the source of the materials; the microfibrils can form into different arrangements[150] resulting in materials with diverse physical properties which make cellulosic materials interesting for developing different biomaterials for biomedical applications. For applications as replacement tissues such as menisci or heart valves, the material needs to be nondegradable, while in tissue engineering applications such as bone scaffolding a biodegradable material is preferred. Biodegradation of cellulosic materials is normally performed in the presence of cellulolytic microorganisms which produces enzymes such as cellobiohydrolases or endoglucanases–glucosidases which can depolymerize cellulose further break it down into free glucose molecules. These cellulolytic enzymes do not exist in humans and therefore native cellulose can be considered nondegradable or slowly degradable in the human body.

Nevertheless, the degree of degradation depends on materials parameters such as crystallinity and hydration of the materials. An early in vivo study[151] reported the importance of cellulose crystallinity and the chemical structure of the cellulose for its degradability. No resorption was observed for samples with higher crystallinity even after six weeks of implantation, while in the case of samples with lower crystallinity, about 50% resorption was observed after four weeks. In another study,[152] the biodegradability of cellulose macro fibers and nanowhiskers was evaluated using a closed bottle test method up to 28 days. This test is based on monitoring the consumption of oxygen in the test solution and is comparable with the theoretical oxygen demand. Cellulose nanowhiskers reached a plateau of biodegrada-

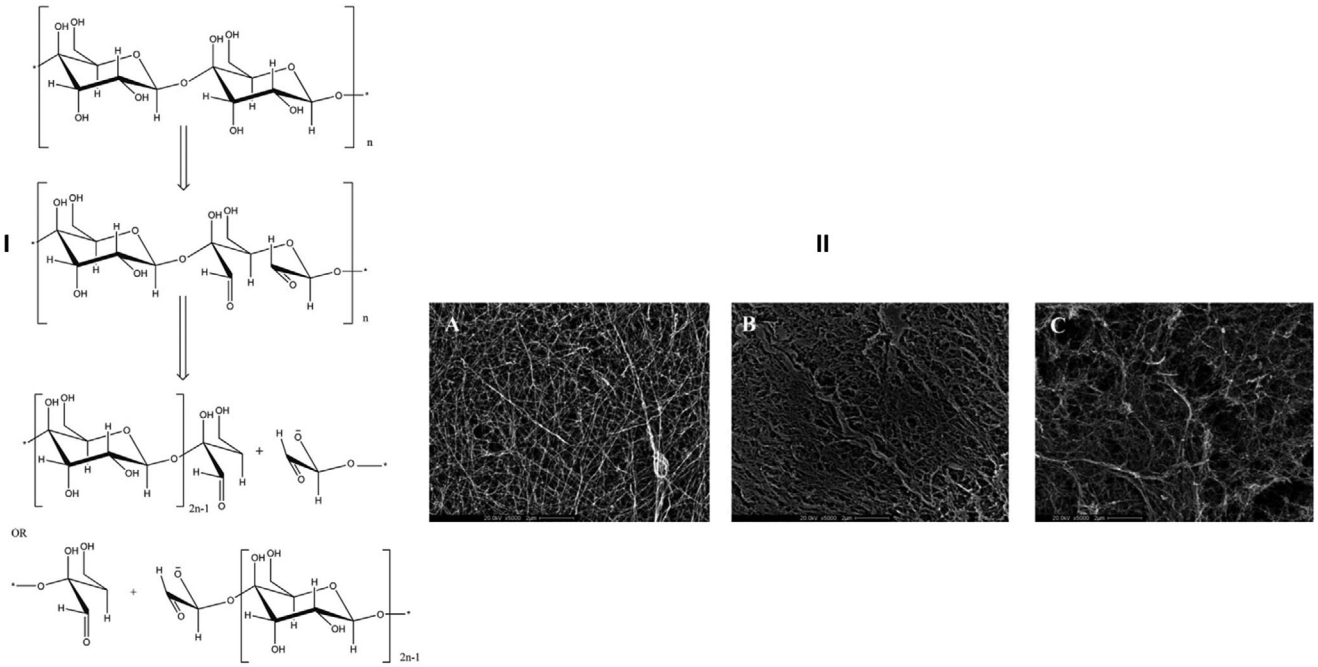

Figure 17. I). Schematic diagram dialdehyde cellulose formation and degradation.[156] II) SEM images of A) native cellulose, B) nonradiated, oxidized cellulose, and C) preirradiated, oxidized cellulose.[157] Reproduced with permission.[157] Copyright 2014, Elsevier.

tion around 54% (after 28 days) while in the case of cellulose fiber the degradation rate was slower, and biodegradation of 45% observed after 28 days while a plateau was not reached. The authors indicated that the higher crystallinity of the cellulose nano whiskers in compared to the cellulose microfiber samples had no effect on its rate of degradation. In the case of methylcellulose, it is regarded to have a higher biodegradation rate as a result of improved water solubility. Through modification of functional groups it is possible to synthesize hydroxypropyl methylcellulose (HPMC) and carboxy methylcellulose (CMC) which in compared to MC are more prone to enzymatic degradation;[153] these have been also used for 3D printing.[154] Nevertheless, as for other cellulosic materials, the human body lacks the cellulase enzyme required to degrade these modified MCs, and therefore its resorption in the human or animal tissue does not occur. To address this issue, in some studies cellulase (cellulose-degrading enzymes) were incorporated in the cellulosic biomaterial such as skin wound dressing to facilitate the biosorption.[155] However, enzymes are pH sensitive, and the changes in the pH of tissues such as skin wounds make the development of practical enzyme containing biomaterials a real challenge. Cellulases can breakdown cellulose without having a negative effect on animal cells. Lou et al. achieved a good hPSC cell propagation in a 3D culture prepared from CNF using cellulase enzyme (200–500 μg g^{-1} of cellulose), which also facilitated the removal of CNF hydrogel resulting in 3D cell spheroids.[155a] The oxidized version of cellulose, 2,3-dialdehyde cellulose (DAC), is more susceptible to hydrolysis and biodegradation in the human body. Oxidation of cellulose with periodate results in the cleavage of C2–C3 bond of the glucopyranoside ring and as a result, two aldehyde groups are formed per unit of glucose (**Figure 17**).[156] At physiological pH, DAC degrades into glycolic acid and 2,4-dihydroxy butyric acid, which are both biodegradable and biocompatible.[157] The glycolic acid in mammals is secreted in the urine and enters the tricarboxylic acid cycle. 2,4-Dihydroxy butyric acid is known to be involved in the metabolism of L-homoserine in the liver.[156] It is worth noting that the oxidization of cellulose with periodate can damage the ordered structure of cellulose nanofiber and lower its crystallinity, which results in its faster degradation, and lower mechanical properties in comparison to nonoxidized cellulose. TEMPO oxidation on the other hand occurs in the disordered region of the cellulose, and by formation of interacetal linkages causes partial reduction of the disordered region, increasing crystallinity. In addition, TEMPO oxidation does not alter the morphology or arrangement of the cellulose fibers. Czaja et al. γ-irradiated (22.5–29 kGy) bacterial cellulose samples followed by periodate oxidation.[157] The SEM images (Figure 17II) indicated that the samples subjected to irradiation followed by oxidization had a disordered structure with dispersed microfibrils in comparison to the native cellulose, which had a more packed fibrillar structure. The samples were subcutaneously implanted in male New Zealand white rabbits, and the biodegradation of the cellulose samples was tested. The results indicated degradation of the preirradiated oxidized cellulose samples as fast as two weeks.

4.3. Sterilization

Sterilization is a critical step in the preparation of biomaterials, including inks and hydrogels, that are used for 3D bioprinting to meet the hygienic requirements of medical devices. Biopolymeric biomaterials usually are sensitive to traditional sterilization methods such as ethylene oxide treatment, gamma irradiation, and steam sterilization. Hodder and co-workers eval-

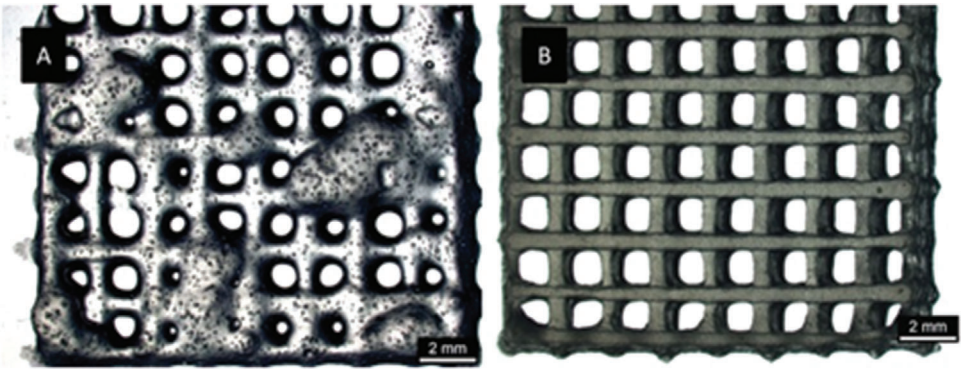

Figure 18. Plotted strands of methyl cellulose (MC)/alginate paste (3:1), 9 × 9 strands, strand width 0.78 mm: A) gamma-irradiated MC and B) $scCO_2$ sterilized MC.[158] Reprinted with permission of a creative commons license.[158] Copyright 2015, the Authors. Published by PLoS One.

uated the effect of autoclave, gamma irradiation, supercritical CO_2 (sCO_2), and UV treatment for the sterilization of methylcellulose as a standard component of bioink such as methylcellulose/alginate ink. Gamma irradiation had a significant effect on the viscosity of the material, which reduced the molecular weight and rendered it unsuitable for 3D bioprinting. While UV treatment and autoclaving showed the best result with regards to cell survival and production of proteoglycan, sCO_2 treatment on the other hand had a negative impact on cell survival. This indicates the importance of the optimization of sCO_2 for its application as a sterilization approach. The residual chemical additives such as acetic acid and hydrogen peroxide that are sometimes added as cosolvent during the sCO_2 sterilization might result in the observed negative cell viability. Therefore, one way is to leave the samples in controlled air condition until these chemicals are removed before using the biomaterials in contact with cells. It is therefore important to consider the specific physicochemical properties of the cellulosic based polymer to better decide on the sterilization method of cellulosic bioinks for biomaterials engineering applications.[37] In another study, Bernhardt et al.[158] developed a $ScCO_2$ using 0.25% water, 0.5% acetic anhydride, and 0.15% hydrogen peroxide for sterilization of methylcellulose – and collagen-based biomaterials. For this purpose, a solution of 9% methylcellulose and 3% alginate was prepared. The $scCO_2$ sterilization could successfully inactivate a large range of microorganisms including endospores of bacteria even when embedded inside the 3D constructs. In addition, the rheological properties of the material were not affected by the $scCO_2$ sterilization process, while gamma irradiation significantly reduced the viscosity of the paste,[158,159] and steam sterilization was not feasible as elevated temperature cause gelation and agglutination of the methylcellulose/alginate material. The sterilized pastes were 3D bioprinted, followed by crosslinking with 100×10^{-3} M $CaCl_2$ solution. The $scCO_2$ treated samples could be homogenously bioprinted and formed stable structures, which was not similarly possible with the gamma sterilized MC pastes (**Figure 18**).

5. Outlook and Conclusions

There is a high and growing demand for green materials and products, whilst the advance of 3D printing relies on a larger range of materials becoming available. This highlights the unique position of lignocellulosic materials for the fabrication of sustainable products with functionalized and customized structures. 3D printing is maturing, and it is now possible to design and fabricate a wide range of 3D-printed lignocellulosic based materials. Our ability to better understand these materials at the molecular scale is growing, allowing us to control their structure, understand their surface properties, and tune their interaction with other materials or physiological environment, which will eventually allow us to design and develop effective materials. This review illustrates the current status of lignocellulosic materials in 3D bioprinting applications. It can be noted that the focus of the current research is largely on cellulose nanofibers, and the majority of the developed inks for 3D bioprinting contain low content (<10%) of nanocellulose. This can be due to increased viscosity of the ink at higher concentrations. Addressing this issue in the near future can result in the development of materials with new physicochemical properties. Additionally, a set of general criteria and standard methods required to better assess the printability of the lignocellulosic based inks for 3D printing will have to be developed.

In terms of a material to reinforce the printed structure, the cellulosic materials and their derivatives have been used to compensate the weakness of polymers such as alginate and gelatin. In this regard, MBC would be a more suitable choice compared to CNF as MBC microfibrils have higher crystallinity and are longer and wider than CNF. Nevertheless, preparing a well dispersed MBC can be also problematic. While there are both chemical techniques based on hydrolysis and physical approaches such as aqueous counter collision method, there might be batch-to-batch variation in terms of particle size and distribution, and the process to eliminate the potential endotoxins from bacteria can be strenuous. In addition, while in many studies CNC has been used for 3D bioprinting of biomaterials there is a lack of focus on the CNC isolation method and its potential effect on the final physiochemical and biological activities of the printed scaffolds. In many studies CNC was sourced commercially, and in commercial industry-scale processes, sulfuric acid hydrolysis is the most common technique. While this method results in material with sulfate half-ester charged groups which impart colloidal stability and facile water processing, other methods such as oxidation, or other acids such as citric, hydrochloric, oxalic and phosphoric acid, can be used for the CNC isolation. There is possibility

and potential to fine-tune the CNC particle size, thermal and colloidal stability, and its surface charge through the choice of the acid which has been left unexplored in the field of 3D printing for biomaterials engineering and biomedical applications. The choice of the acid and reaction process can be tailored depending on the exact requirement of the printed material's properties, and its final application instead of using the commercially produced CNC. Moreover, efficient, green solvents are needed to achieve homogeneous cellulosic based solutions that can be functionalized for the better formulation of biomaterial inks with potential to outperform or replace current materials such as alginate and gelatin. Considering the slow biodegradation, the 3D-structured cellulosic materials can be considered for reparative applications such as wound dressing while more studies need to be performed before applying these compounds as long-term implants for regenerative applications, as they may cause chronic inflammation and foreign body response. Furthermore, in order to achieve 3D-printed lignocellulosic materials at industrial scale, the technological barrier concerning the rate of printing need to be resolved. Considering the range of its potential applications, it is highly predictable that those barriers will soon be tackled.

Conflict of Interest

The authors declare no conflict of interest.

Keywords

biofabrication, bioinks, cellulose, hemicellulose, hydrogels, lignin

Received: August 19, 2020
Revised: October 1, 2020
Published online:

[1] P. Tack, J. Victor, P. Gemmel, L. Annemans, *Biomed. Eng. Online* **2016**, *15*, 115.
[2] L. Moroni, T. Boland, J. A. Burdick, C. De Maria, B. Derby, G. Forgacs, J. Groll, Q. Li, J. Malda, V. A. Mironov, C. Mota, M. Nakamura, W. Shu, S. Takeuchi, T. B. F. Woodfield, T. Xu, J. J. Yoo, G. Vozzi, *Trends Biotechnol.* **2018**, *36*, 384.
[3] L. Valot, J. Martinez, A. Mehdi, G. Subra, *Chem. Soc. Rev.* **2019**, *48*, 4049.
[4] J. Groll, J. A. Burdick, D. W. Cho, B. Derby, M. Gelinsky, S. C. Heilshorn, T. Jüngst, J. Malda, V. A. Mironov, K. Nakayama, A. Ovsianikov, W. Sun, S. Takeuchi, J. J. Yoo, T. B. F. Woodfield, *Biofabrication* **2018**, *11*, 013001.
[5] L. Moroni, J. A. Burdick, C. Highley, S. J. Lee, Y. Morimoto, S. Takeuchi, J. J. Yoo, *Nat. Rev. Mater.* **2018**, *3*, 21.
[6] J. Malda, J. Visser, F. P. Melchels, T. Jüngst, W. E. Hennink, W. J. A. Dhert, J. Groll, D. W. Hutmacher, *Adv. Mater.* **2013**, *25*, 5011.
[7] J. Groll, T. Boland, T. Blunk, J. A. Burdick, D.-W. Cho, P. D. Dalton, B. Derby, G. Forgacs, Q. Li, V. A. Mironov, L. Moroni, M. Nakamura, W. Shu, S. Takeuchi, G. Vozzi, T. B. F. Woodfield, T. Xu, J. J. Yoo, J. Malda, *Biofabrication* **2016**, *8*, 013001.
[8] C. Moser, G. Henriksson, M. E. Lindström, **2016**, *11*, 9.
[9] R. J. Moon, A. Martini, J. Nairn, J. Simonsen, J. Youngblood, *Chem. Soc. Rev.* **2011**, *40*, 3941.
[10] a) W. Xu, X. Wang, N. Sandler, S. Willför, C. Xu, *ACS Sustainable Chem. Eng.* **2018**, *6*, 5663; b) L. Dai, T. Cheng, C. Duan, W. Zhao, W. Zhang, X. Zou, J. Aspler, Y. Ni, *Carbohydr. Polym.* **2019**, *203*, 71; c) D. Klemm, E. D. Cranston, D. Fischer, M. Gama, S. A. Kedzior, D. Kralisch, F. Kramer, T. Kondo, T. Lindström, S. Nietzsche, K. Petzold-Welcke, F. Rauchfuß, *Mater. Today* **2018**, *21*, 720; d) H. Du, W. Liu, M. Zhang, C. Si, X. Zhang, B. Li, *Carbohydr. Polym.* **2019**, *209*, 130.
[11] S. Loai, B. R. Kingston, Z. Wang, D. N. Philpott, M. Tao, H.-L. M. Cheng, *Regener. Med. Front.* **2019**, *1*, e190004.
[12] M. Jonoobi, R. Oladi, Y. Davoudpour, K. Oksman, A. Dufresne, Y. Hamzeh, R. Davoodi, *Cellulose* **2015**, *22*, 935.
[13] M. Tayyab, A. Noman, W. Islam, S. Waheed, Y. Arafat, F. Ali, M. Zaynab, S. Lin, H. Zhang, W. Lin, *Appl. Ecol. Env. Res.* **2017**, *16*, 225.
[14] a) T. H. Jovic, G. Kungwengwe, A. C. Mills, I. S. Whitaker, *Front. Mech. Eng.* **2019**, *5*, 1. b) R. Curvello, V. S. Raghuwanshi, G. Garnier, *Adv. Colloid Interface Sci.* **2019**, *267*, 47; c) M. W. Ullah, L. Fu, L. Lamboni, Z. Shi, G. Yang, in *Materials for Biomedical Engineering: Absorbable Polymers*, Elsevier, Amsterdam **2018**, p. 41.
[15] a) K. Higashi, N. Miki, *Micromachines* **2018**, *9*, 36; b) L.-M. Papaspyridi, A. Zerva, E. Topakas, *Catalysts* **2018**, *8*, 274; c) F. Esa, S. M. Tasirin, N. A. Rahman, *Agric. Agric. Sci. Proc.* **2014**, *2*, 113.
[16] R. M. Brown, Jr, *J. Macromol. Sci., Part A: Pure Appl. Chem.* **1996**, *33*, 1345.
[17] X. Xu, F. Liu, L. Jiang, J. Y. Zhu, D. Haagenson, D. P. Wiesenborn, *ACS Appl. Mater. Interfaces* **2013**, *5*, 2999.
[18] D. A. Gopakumar, S. Thomas, Y. Grohens, in *Multifunctional Polymeric Nanocomposites Based on Cellulosic Reinforcements* (Eds: D. Puglia, E. Fortunati, J. M. Kenny), William Andrew Publishing, Norwich, NY **2016**, p. 253.
[19] N. Lin, A. Dufresne, *Eur. Polym. J.* **2014**, *59*, 302.
[20] J. George, S. N. Sabapathi, *Nanotechnol., Sci. Appl.* **2015**, *8*, 45.
[21] T. Abitbol, D. Kam, Y. Levi-Kalisman, D. G. Gray, O. Shoseyov, *Langmuir* **2018**, *34*, 3925.
[22] S. Varanasi, L. Henzel, L. Mendoza, R. Prathapan, W. Batchelor, R. Tabor, G. Garnier, *Front. Chem.* **2018**, *6*, 6.
[23] M. A. Usmani, I. Khan, U. Gazal, M. K. Mohamad Haafiz, A. H. Bhat, in *Polymer-Based Nanocomposites for Energy and Environmental Applications* (Eds: M. Jawaid, M. M. Khan), Woodhead Publishing, Cambridge, UK **2018**, p. 441.
[24] F. Ansari, L. A. Berglund, in *Multifunctional Polymeric Nanocomposites Based on Cellulosic Reinforcements* (Eds: D. Puglia, E. Fortunati, J. M. Kenny), William Andrew Publishing, Norwich, NY **2016**, p. 115.
[25] S. Otto, H. Synnøve, M. Ali, S. Borregaard, *Coatings World* **2019**. https://www.coatingsworld.com/issues/2019-06-01/view_technical-papers/microfibrillated-cellulose-a-novel-and-renewablemultifunctional-additive-for-waterborne-coatings/
[26] a) F. W. Herrick, R. L. Casebier, J. K. Hamilton, K. R. Sandberg, *J. Appl. Polym. Sci.: Appl. Polym. Symp.* **1983**, *37*, 797. b) I. Siró, D. Plackett, *Cellulose* **2010**, *17*, 459.
[27] B. Wu, B. Geng, Y. Chen, H. Liu, G. Li, Q. Wu, *Front. Chem. Sci. Eng.* **2017**, *11*, 554.
[28] H. Fukuzumi, T. Saito, A. Isogai, *Carbohydr. Polym.* **2013**, *93*, 172.
[29] a) H. L.e Van, Z. Lindong, K. J. Woong, C. Eun-sik, K. Jaehwan, *Proc. SPIE* **2017**, https://doi.org/10.1117/12.2259841. b) M. Wakabayashi, S. Fujisawa, T. Saito, A. Isogai, *Front. Chem.* **2020**, https://doi.org/10.3389/fchem.2020.00037. c) A. Isogai, T. Saito, H. Fukuzumi, *Nanoscale* **2011**, *3*, 71.
[30] D. Klemm, F. Kramer, S. Moritz, T. Lindström, M. Ankerfors, D. Gray, A. Dorris, *Angew. Chem., Int. Ed.* **2011**, *50*, 5438.
[31] N. Contessi Negrini, L. Bonetti, L. Contili, S. Farè, *Bioprinting* **2018**, *10*, e00024.
[32] S. Paul, M. Gupta, *Tetrahedron Lett.* **2004**, *45*, 8825.
[33] D. Ye, D. Montané, X. Farriol, *Carbohydr. Polym.* **2005**, *61*, 446.
[34] T. Ahlfeld, V. Guduric, S. Duin, A. R. Akkineni, K. Schütz, D. Kilian, J. Emmermacher, N. Cubo-Mateo, S. Dani, M. v. Witzleben, J. Span-

genberg, R. Abdelgaber, R. F. Richter, A. Lode, M. Gelinsky, *Biomater. Sci.* **2020**, *8*, 2102.
[35] C. Chemicalbook, **2020**.
[36] N. Sarkar, *Carbohydr. Polym.* **1995**, *26*, 195.
[37] E. Hodder, S. Duin, D. Kilian, T. Ahlfeld, J. Seidel, C. Nachtigall, P. Bush, D. Covill, M. Gelinsky, A. Lode, *J. Mater. Sci.: Mater. Med.* **2019**, *30*, 10.
[38] J. Brady, T. Dürig, P. I. Lee, J. X. Li, in *Developing Solid Oral Dosage Forms*, 2nd ed. (Eds: Y. Qiu, Y. Chen, G. G. Z. Zhang, L. Yu, R. V. Mantri), Academic Press, Boston, MA **2017**, p. 181.
[39] P. L. Nasatto, F. Pignon, J. L. M. Silveira, M. E. R. Duarte, M. D. Noseda, M. Rinaudo, *Polymers* **2015**, *7*, 777.
[40] N. Contessi, L. Altomare, A. Filipponi, S. Farè, *Mater. Lett.* **2017**, *207*, 157.
[41] K. Schütz, A.-M. Placht, B. Paul, S. Brüggemeier, M. Gelinsky, A. Lode, *J. Tissue Eng. Regener. Med.* **2017**, *11*, 1574.
[42] N. Law, B. Doney, H. Glover, Y. Qin, Z. M. Aman, T. B. Sercombe, L. J. Liew, R. J. Dilley, B. J. Doyle, *J. Mech. Behav. Biomed. Mater.* **2018**, *77*, 389.
[43] C.-H. Chen, Y. Chang, C.-C. Wang, C.-H. Huang, C.-C. Huang, Y.-C. Yeh, S.-M. Hwang, H.-W. Sung, *Biomaterials* **2007**, *28*, 4643.
[44] a) H. Zhang, X. Xu, C. Chen, X. Chen, Y. Huang, D. Sun, *Mater. Lett.* **2019**, *249*, 104; b) A. F. Jozala, L. C. de Lencastre-Novaes, A. M. Lopes, V. de Carvalho Santos-Ebinuma, P. G. Mazzola, A. Pessoa, Jr, D. Grotto, M. Gerenutti, M. V. Chaud, *Appl. Microbiol. Biotechnol.* **2016**, *100*, 2063; c) S. Khan, M. Ul-Islam, M. Ikram, M. W. Ullah, M. Israr, F. Subhan, Y. Kim, J. H. Jang, S. Yoon, J. K. Park, *RSC Adv.* **2016**, *6*, 110840.
[45] M. V. Zugravu, R. A. Smith, B. T. Reves, J. A. Jennings, J. O. Cooper, W. O. Haggard, J. D. Bumgardner, *J. Biomater. Appl.* **2013**, *28*, 566.
[46] a) T. R. Stumpf, X. Yang, J. Zhang, X. Cao, *Mater. Sci. Eng., C* **2018**, *82*, 372; b) H. G.de Oliveira Barud, R. R. da Silva, H. da Silva Barud, A. Tercjak, J. Gutierrez, W. R. Lustri, O. B. de Oliveira Junior, S. J. Ribeiro, *Carbohydr. Polym.* **2016**, *153*, 406; c) E. Liyaskina, V. Revin, E. Paramonova, M. Nazarkina, N. Pestov, N. Revina, S. Kolesnikova, *J. Phys.: Conf. Ser.* **2017**, *784*, https://doi.org/10.1088/1742-6596/784/1/012034 d) A. Blanco, M. C. Monte, C. Campano, A. Balea, N. Merayo, C. Negro, in *Handbook of Nanomaterials for Industrial Applications*, (Ed: M. H. Chaudhery), Elsevier, Amsterdam **2018**, p. 74; e) J. Wang, J. Tavakoli, Y. Tang, *Carbohydr. Polym.* **2019**, *219*, 63 f) M. Reza, C. Bertinetto, K. K. Kesari, P. Engelhardt, J. Ruokolainen, T. Vuorinen, *Sci. Rep.* **2019**, *9*, 3869; g) A. R. Rebelo, A. J. Archer, X. Chen, C. Liu, G. Yang, Y. Liu, *Sci. Technol. Adv. Mater.* **2018**, *19*, 203.
[47] M. Liu, L. Liu, S. Jia, S. Li, Y. Zou, C. Zhong, *Sci. Rep.* **2018**, *8*, 6266.
[48] L. Salgado, S. Blank, R. A. M. Esfahani, J. L. Strap, D. Bonetta, *BMC Microbiol.* **2019**, *19*, 216.
[49] V. Revin, E. Liyaskina, M. Nazarkina, A. Bogatyreva, M. Shchankin, *Braz. J. Microbiol.* **2018**, *49*, 151.
[50] E. Tsouko, C. Kourmentza, D. Ladakis, N. Kopsahelis, I. Mandala, S. Papanikolaou, F. Paloukis, V. Alves, A. Koutinas, *Int. J. Mol. Sci.* **2015**, *16*, 14832.
[51] A. Pfalzgraff, K. Brandenburg, G. Weindl, *Front. Pharmacol.* **2018**, *9*, 281.
[52] A.-C. Burdusel, O. Gherasim, A. M. Grumezescu, L. Mogoantă, A. Ficai, E. Andronescu, *Nanomaterials* **2018**, *8*, 681.
[53] C. Wiegand, S. Moritz, N. Hessler, D. Kralisch, F. Wesarg, F. A. Müller, D. Fischer, U.-C. Hipler, *J. Mater. Sci.: Mater. Med.* **2015**, *26*, 245.
[54] W. Shao, H. Liu, S. Wang, J. Wu, M. Huang, H. Min, X. Liu, *Carbohydr. Polym.* **2016**, *145*, 114.
[55] S. C. Fernandes, P. Sadocco, A. Alonso-Varona, T. Palomares, A. Eceiza, A. J. Silvestre, I. a. Mondragon, C. S. Freire, *ACS Appl. Mater. Interfaces* **2013**, *5*, 3290.
[56] G. Chantereau, N. Brown, M.-A. Dourges, C. S. Freire, A. J. Silvestre, G. Sebe, V. Coma, *Carbohydr. Polym.* **2019**, *220*, 71.
[57] F. Wahid, Y.-X. Duan, X.-H. Hu, L.-Q. Chu, S.-R. Jia, J.-D. Cui, C. Zhong, *Int. J. Biol. Macromol.* **2019**, *132*, 692.
[58] P. Dhar, B. Pratto, A. J. G. Cruz, S. Bankar, *J. Cleaner Prod.* **2019**, *238*, 117859.
[59] H. V. Scheller, P. Ulvskov, *Annu. Rev. Plant Biol.* **2010**, *61*, 263.
[60] J. Bian, F. Peng, X. Peng, F. Xu, R. Sun, J. F. Kennedy, *Carbohydr. Polym.* **2012**, *88*, 638.
[61] K. Kucharska, P. Rybarczyk, I. Hołowacz, R. Łukajtis, M. Glinka, M. Kamiński, *Molecules* **2018**, *23*, 2937.
[62] K. M. Davis, M. Rover, R. C. Brown, X. Bai, Z. Wen, L. R. Jarboe, *Energies* **2016**, *9*, 808.
[63] J. C. Río, A. G. Lino, J. L. Colodette, C. F. Lima, A. Gutiérrez, A. T. Martínez, F. Lu, J. Ralph, J. Rencoret, *Biomass Bioenergy* **2015**, *81*, 322.
[64] B. Lochab, S. Shukla, I. K. Varmab, *RSC Adv.* **2014**, *4*, 21712.
[65] J. Liu, L. Sun, W. Xu, Q. Wang, S. Yu, J. Sun, *Carbohydr. Polym.* **2019**, *207*, 297.
[66] M. K. Hausmann, P. A. Rühs, G. Siqueira, J. Läuger, R. Libanori, T. Zimmermann, A. R. Studart, *ACS Nano* **2018**, *12*, 6926.
[67] A. Schwab, R. Levato, M. D'Este, S. Piluso, D. Eglin, J. Malda, *Chem. Rev.* **2020**, *120*, 11028.
[68] A. Habib, V. Sathish, S. Mallik, B. Khoda, *Materials* **2018**, *11*, 454.
[69] H. Rastin, R. T. Ormsby, G. J. Atkins, D. Losic, *ACS Appl. Bio Mater.* **2020**, *3*, 1815.
[70] M. Zuo, N. Pan, Q. Liu, X. Ren, Y. Liu, T.-S. Huang, *RSC Adv.* **2020**, *10*, 2952.
[71] J. Leppiniemi, P. Lahtinen, A. Paajanen, R. Mahlberg, S. Metsä-Kortelainen, T. Pinomaa, H. Pajari, I. Vikholm-Lundin, P. Pursula, V. P. Hytönen, *ACS Appl. Mater. Interfaces* **2017**, *9*, 21959.
[72] E. B. Heggset, B. L. Strand, K. W. Sundby, S. Simon, G. Chinga-Carrasco, K. Syverud, *Cellulose* **2019**, *26*, 581.
[73] O. Aarstad, E. B. Heggset, I. S. Pedersen, S. H. Bjornoy, K. Syverud, B. L. Strand, *Polymers* **2017**, *9*, 378.
[74] H. Martínez Ávila, S. Schwarz, N. Rotter, P. Gatenholm, *Bioprinting* **2016**, *1–2*, 22.
[75] N. B. Palaganas, J. D. Mangadlao, A. C. C. de Leon, J. O. Palaganas, K. D. Pangilinan, Y. J. Lee, R. C. Advincula, *ACS Appl. Mater. Interfaces* **2017**, *9*, 34314.
[76] V. Kuzmenko, E. Karabulut, E. Pernevik, P. Enoksson, P. Gatenholm, *Carbohydr. Polym.* **2018**, *189*, 22.
[77] E. Campodoni, E. B. Heggset, A. Rashad, G. B. Ramírez-Rodríguez, K. Mustafa, K. Syverud, A. Tampieri, M. Sandri, *Mater. Sci. Eng., C* **2019**, *94*, 867.
[78] W. Xu, B. Z. Molino, F. Cheng, P. J. Molino, Z. Yue, D. Su, X. Wang, S. Willför, C. Xu, G. G. Wallace, *ACS Appl. Mater. Interfaces* **2019**, *11*, 8838.
[79] R.-D. Chen, C.-F. Huang, S.-h. Hsu, *Carbohydr. Polym.* **2019**, *212*, 75.
[80] W. Leng, J. Li, Z. Cai, *Polymers* **2017**, *9*, 597.
[81] D. Kam, M. Chasnitsky, C. Nowogrodski, I. Braslavsky, T. Abitbol, S. Magdassi, O. Shoseyov, *Colloids Interfaces* **2019**, *3*, 46.
[82] L. Lewis, S. G. Hatzikiriakos, W. Y. Hamad, M. J. MacLachlan, *ACS Macro Lett.* **2019**, *8*, 486.
[83] M. Ojansivu, A. Rashad, A. Ahlinder, J. Massera, A. Mishra, K. Syverud, A. Finne-Wistrand, S. Miettinen, K. Mustafa, *Biofabrication* **2019**, *11*, 035010.
[84] a) C. Jia, F. Jiang, P. Hu, Y. Kuang, S. He, T. Li, C. Chen, A. Murphy, C. Yang, Y. Yao, J. Dai, C. B. Raub, X. Luo, L. Hu, *ACS Appl. Mater. Interfaces* **2018**, *10*, 7362; b) J. Li, X. Liu, E. Tomaskovic-Crook, J. M. Crook, G. G. Wallace, *Colloids Surf., B* **2019**, *176*, 87.
[85] a) H. Li, Y. J. Tan, K. F. Leong, L. Li, *ACS Appl. Mater. Interfaces* **2017**, *9*, 20086; b) T. Ahlfeld, G. Cidonio, D. Kilian, S. Duin, A. R. Akkineni,

J. I. Dawson, S. Yang, A. Lode, R. O. C. Oreffo, M. Gelinsky, *Biofabrication* **2017**, *9*, 034103.
[86] J. Y. Shin, Y. H. Yeo, J. E. Jeong, S. A. Park, W. H. Park, *Carbohydr. Polym.* **2020**, *238*, 116192.
[87] D. Kilian, T. Ahlfeld, A. R. Akkineni, A. Bernhardt, M. Gelinsky, A. Lode, *Sci. Rep.* **2020**, *10*, 8277.
[88] D. Caccavo, S. Cascone, G. Lamberti, A. Barba, *Chem. Soc. Rev.* **2018**, *47*, 2357.
[89] X. Lv, C. Feng, Y. Liu, X. Peng, S. Chen, D. Xiao, H. Wang, Z. Li, Y. Xu, M. Lu, *Theranostics* **2018**, *8*, 3153.
[90] M. L. Foresti, A. Vázquez, B. Boury, *Carbohydr. Polym.* **2017**, *157*, 447.
[91] S. Napavichayanun, R. Yamdech, P. Aramwit, *Int. J. Polym. Mater. Polym. Biomater.* **2018**, *67*, 61.
[92] A. Azarniya, N. Eslahi, N. Mahmoudi, A. Simchi, *Composites, Part A* **2016**, *85*, 113.
[93] a) C.-H. Su, G. V. Kumar, S. Adhikary, P. Velusamy, K. Pandian, P. Anbu, *Biochem. Eng. J.* **2017**, *117*, 28; b) W. Shao, H. Liu, X. Liu, S. Wang, J. Wu, R. Zhang, H. Min, M. Huang, *Carbohydr. Polym.* **2015**, *132*, 351.
[94] Y. Li, H. Jiang, W. Zheng, N. Gong, L. Chen, X. Jiang, G. Yang, *J. Mater. Chem. B* **2015**, *3*, 3498.
[95] I. M. Araújo, R. R. Silva, G. Pacheco, W. R. Lustri, A. Tercjak, J. Gutierrez, J. R. Júnior, F. H. Azevedo, G. S. Figuêredo, M. L. Vega, *Carbohydr. Polym.* **2018**, *179*, 341.
[96] S. Ye, L. Jiang, C. Su, Z. Zhu, Y. Wen, W. Shao, *Int. J. Biol. Macromol.* **2019**, *133*, 148.
[97] Y.-m. Cao, M.-y. Liu, Z.-w. Xue, Y. Qiu, J. Li, Y. Wang, Q.-k. Wu, *Biochem. Biophys. Res. Commun.* **2019**, *516*, 1167.
[98] P. A. Rühs, F. Storz, Y. A. López Gómez, M. Haug, P. Fischer, *npj Biofilms Microbiomes* **2018**, *4*, 21.
[99] P. Apelgren, E. Karabulut, M. Amoroso, A. Mantas, H. Martínez Ávila, L. Kölby, T. Kondo, G. Toriz, P. Gatenholm, *ACS Biomater. Sci. Eng.* **2019**, *5*, 2482.
[100] E. Altun, N. Ekren, S. E. Kuruca, O. Gunduz, *Mater. Lett.* **2019**, *234*, 163.
[101] B. F. Bergel, S. D. Osorio, L. M. da Luz, R. M. C. Santana, *Carbohydr. Polym.* **2018**, *200*, 106.
[102] M. M. Hassan, M. J. Le Guen, N. Tucker, K. Parker, *Cellulose* **2019**, *26*, 4463.
[103] X. Zhang, J. Zhou, J. Chen, B. Li, Y. Li, S. Liu, *Food Hydrocolloids* **2020**, *100*, 105440.
[104] I. Sulaeva, H. Hettegger, A. Bergen, C. Rohrer, M. Kostic, J. Konnerth, T. Rosenau, A. Potthast, *Mater. Sci. Eng., C* **2020**, *110*, 110619.
[105] J. Liu, G. Chinga-Carrasco, F. Cheng, W. Xu, S. Willför, K. Syverud, C. Xu, *Cellulose* **2016**, *23*, 3129.
[106] W. Xu, X. Zhang, P. Yang, O. Långvik, X. Wang, Y. Zhang, F. Cheng, M. Österberg, S. Willför, C. Xu, *ACS Appl. Mater. Interfaces* **2019**, *11*, 12389.
[107] K. Markstedt, A. Escalante, G. Toriz, P. Gatenholm, *ACS Appl. Mater. Interfaces* **2017**, *9*, 40878.
[108] C. V. Cerclier, A. l. Guyomard-Lack, F. Cousin, B. Jean, E. Bonnin, B. Cathala, C. l. Moreau, *Biomacromolecules* **2013**, *14*, 3599.
[109] A. Dammak, C. Moreau, F. Azzam, B. Jean, F. Cousin, B. Cathala, *J. Colloid Interface Sci.* **2015**, *460*, 214.
[110] J. Hanus, K. Mazeau, *Biopolymers* **2006**, *82*, 59.
[111] H. Sehaqui, M. Salajková, Q. Zhou, L. A. Berglund, *Soft Matter* **2010**, *6*, 1824.
[112] S. Josset, L. Hansen, P. Orsolini, M. Griffa, O. Kuzior, B. Weisse, T. Zimmermann, T. Geiger, *Cellulose* **2017**, *24*, 3825.
[113] W. Xu, A. Pranovich, P. Uppstu, X. Wang, D. Kronlund, J. Hemming, H. Öblom, N. Moritz, M. Preis, N. Sandler, S. Willför, C. Xu, *Carbohydr. Polym.* **2018**, *187*, 51.
[114] T. Köhnke, T. Elder, H. Theliander, A. J. Ragauskas, *Carbohydr. Polym.* **2014**, *100*, 24.
[115] L. Berglund, F. Forsberg, M. Jonoobi, K. Oksman, *RSC Adv.* **2018**, *8*, 38219.
[116] L. Wu, S. Huang, J. Zheng, Z. Qiu, X. Lin, Y. Qin, *Int. J. Biol. Macromol.* **2019**, *140*, 538.
[117] J. Simon, E. Flahaut, M. Golzio, *Materials* **2019**, *12*, 624.
[118] E.-S. Lee, Y.-O. Kim, Y.-M. Ha, D. Lim, J. Y. Hwang, J. Kim, M. Park, J. W. Cho, Y. C. Jung, *Eur. Polym. J.* **2018**, *105*, 79.
[119] Y. Zhang, M. Jiang, Y. Zhang, Q. Cao, X. Wang, Y. Han, G. Sun, Y. Li, J. Zhou, *Mater. Sci. Eng., C* **2019**, *104*, 110002.
[120] G. Jaganathan, K. Manivannan, S. Lakshmanan, M. A. Sithique, *Sustainable Chem. Pharm.* **2018**, *10*, 27.
[121] K. R. Aadil, S. I. Mussatto, H. Jha, *Int. J. Biol. Macromol.* **2018**, *120*, 763.
[122] S. Yoon, J. A. Park, H. R. Lee, W. H. Yoon, D. S. Hwang, S. Jung, *Adv. Healthcare Mater.* **2018**, *7*, 1800050.
[123] M. Milojević, L. Gradišnik, J. Stergar, M. Skelin Klemen, A. Stožer, M. Vesenjak, P. Dobnik Dubrovski, T. Maver, T. Mohan, K. Stana Kleinschek, U. Maver, *Appl. Surf. Sci.* **2019**, *488*, 836.
[124] C. Xu, B. Zhang Molino, X. Wang, F. Cheng, W. Xu, P. Molino, M. Bacher, D. Su, T. Rosenau, S. Willför, G. Wallace, *J. Mater. Chem. B* **2018**, *6*, 7066.
[125] I. Henriksson, P. Gatenholm, D. A. Hägg, *Biofabrication* **2017**, *9*, 015022.
[126] T. Möller, M. Amoroso, D. Hägg, C. Brantsing, N. Rotter, P. Apelgren, A. Lindahl, L. Kölby, P. Gatenholm, *Plastic and Reconstructive Surgery—Global Open*, Vol. *5*, Wolters Kluwer, Dordrecht, The Netherlands **2017**, p. e1227.
[127] M. Müller, E. Öztürk, Ø. Arlov, P. Gatenholm, M. Zenobi-Wong, *Ann. Biomed. Eng.* **2017**, *45*, 210.
[128] D. Nguyen, D. A. Hägg, A. Forsman, J. Ekholm, P. Nimkingratana, C. Brantsing, T. Kalogeropoulos, S. Zaunz, S. Concaro, M. Brittberg, A. Lindahl, P. Gatenholm, A. Enejder, S. Simonsson, *Sci. Rep.* **2017**, *7*, 658.
[129] G. Chinga-Carrasco, N. V. Ehman, D. Filgueira, J. Johansson, M. E. Vallejos, F. E. Felissia, J. Håkansson, M. C. Area, *Addit. Manuf.* **2019**, *28*, 267.
[130] R. Ajdary, S. Huan, N. Zanjanizadeh Ezazi, W. Xiang, R. Grande, H. A. Santos, O. J. Rojas, *Biomacromolecules* **2019**, *20*, 2770.
[131] S. Shin, H. Kwak, J. Hyun, *Carbohydr. Polym.* **2019**, *225*, 115235.
[132] E. Prince, M. Alizadehgiashi, M. Campbell, N. Khuu, A. Albulescu, K. De France, D. Ratkov, Y. Li, T. Hoare, E. Kumacheva, *Biomacromolecules* **2018**, *19*, 1276.
[133] Y. Jiang, J. Zhou, H. Shi, G. zhao, Q. Zhang, C. Feng, X. Xv, *J. Mater. Sci.* **2020**, *55*, 2618.
[134] F. Qian, C. Zhu, J. M. Knipe, S. Ruelas, J. K. Stolaroff, J. R. DeOtte, E. B. Duoss, C. M. Spadaccini, C. A. Henard, M. T. Guarnieri, S. E. Baker, *Nano Lett.* **2019**, *19*, 5829.
[135] Y. Wu, Z. Y. Lin, A. C. Wenger, K. C. Tam, X. Tang, *Bioprinting* **2018**, *9*, 1.
[136] Z. M. Jessop, A. Al-Sabah, N. Gao, S. Kyle, B. Thomas, N. Badiei, K. Hawkins, I. S. Whitaker, *Biofabrication* **2019**, *11*, 045006.
[137] L. Huang, X. Du, S. Fan, G. Yang, H. Shao, D. Li, C. Cao, Y. Zhu, M. Zhu, Y. Zhang, *Carbohydr. Polym.* **2019**, *221*, 146.
[138] S. Shin, H. Kwak, D. Shin, J. Hyun, *Nat. Commun.* **2019**, *10*, 4650.
[139] S. Shin, S. Park, M. Park, E. Jeong, K. Na, H. J. Youn, J. Hyun, *BioResources* **2017**, *12*, 2941.
[140] G. Melilli, I. Carmagnola, C. Tonda-Turo, F. Pirri, G. Ciardelli, M. Sangermano, M. Hakkarainen, A. Chiappone, *Polymers* **2020**, *12*, 1655.
[141] B. D. Ratner, in *Host Response to Biomaterials* (Ed: S. F. Badylak), Academic Press, Oxford **2015**, p. 37.

[142] a) F. K. Andrade, N. Alexandre, I. Amorim, F. Gartner, A. C. Maurício, A. L. Luís, M. Gama, *J. Bioact. Compat. Polym.* **2013**, *28*, 97; b) R. A. N. Pértile, S. Moreira, R. M. Gil da Costa, A. Correia, L. Guãrdao, F. Gartner, M. Vilanova, M. Gama, *J. Biomater. Sci., Polym. Ed.* **2012**, *23*, 1339.
[143] N. Yanamala, M. T. Farcas, M. K. Hatfield, E. R. Kisin, V. E. Kagan, C. L. Geraci, A. A. Shvedova, *ACS Sustainable Chem. Eng.* **2014**, *2*, 1691.
[144] J. Catalán, E. Rydman, K. Aimonen, K.-S. Hannukainen, S. Suhonen, E. Vanhala, C. Moreno, V. Meyer, D. d. S. Perez, A. Sneck, U. Forsström, C. Højgaard, M. Willemoes, J. R. Winther, U. Vogel, H. Wolff, H. Alenius, K. M. Savolainen, H. Norppa, *Mutagenesis* **2017**, *32*, 23.
[145] A. Rashad, S. Suliman, M. Mustafa, T. Ø. Pedersen, E. Campodoni, M. Sandri, K. Syverud, K. Mustafa, *Mater. Sci. Eng., C* **2019**, *97*, 208.
[146] A. Shimotoyodome, J. Suzuki, Y. Kumamoto, T. Hase, A. Isogai, *Biomacromolecules* **2011**, *12*, 3812.
[147] G. Helenius, H. Bäckdahl, A. Bodin, U. Nannmark, P. Gatenholm, B. Risberg, *J. Biomed. Mater. Res., Part A* **2006**, *76A*, 431.
[148] F. G. Torres, S. Commeaux, O. P. Troncoso, *J. Funct. Biomater.* **2012**, *3*, 864.
[149] M. Roman, *Ind. Biotechnol.* **2015**, *11*, 25.
[150] George J., S. SN, *Nanotechnol., Sci. Appl.* **2015**, *8*, 45.
[151] T. Miyamoto, S.-i. Takahashi, H. Ito, H. Inagaki, Y. Noishiki, *J. Biomed. Mater. Res.* **1989**, *23*, 125.
[152] K. Kümmerer, J. Menz, T. Schubert, W. Thielemans, *Chemosphere* **2011**, *82*, 1387.
[153] M. G. Wirick, *J. Polym. Sci., Part A-1: Polym. Chem.* **1968**, *6*, 1965.
[154] M. A. Habib, B. Khoda, *Procedia Manuf.* **2018**, *26*, 846.
[155] a) Y. R. Lou, L. Kanninen, T. Kuisma, J. Niklander, L. A. Noon, D. Burks, A. Urtti, M. Yliperttula, *Stem Cells Dev.* **2014**, *23*, 380; b) Y. Hu, J. M. Catchmark, *Acta Biomater.* **2011**, *7*, 2835.
[156] J. Li, Y. Wan, L. Li, H. Liang, J. Wang, *Mater. Sci. Eng., C* **2009**, *29*, 1635.
[157] W. Czaja, D. Kyryliouk, C. A. DePaula, D. D. Buechter, *J. Appl. Polym. Sci.* **2014**, *131*, 39995.
[158] A. Bernhardt, M. Wehrl, B. Paul, T. Hochmuth, M. Schumacher, K. Schütz, M. Gelinsky, *PLoS One* **2015**, *10*, e0129205.
[159] K. H. Matthews, H. N. E. Stevens, A. D. Auffret, M. J. Humphrey, G. M. Eccleston, *Int. J. Pharm.* **2006**, *313*, 78.

Amin Shavandi is an assistant professor in the faculty of engineering, at the free university of Brussels (ULB). His research contributes to the development of new functionalized polymers, fibers, composites, and in particular biomaterials for tissue engineering applications derived from biobased materials and renewable resources, including waste and side streams. Amin has an M.Sc. in chemical engineering and a Ph.D. (2017) in food science–medicine from the University of Otago, New Zealand.

Lei Nie completed his Ph.D. (2013) from Huazhong University of Science and Technology, and after that received three years of postdoctoral training at Ningbo Institute of Materials Technology and Engineering (CAS, China) and Free University of Berlin (Germany). He began his research as an independent PI at Xinyang Normal University (China) in 2017. He started 3D bioprinting work at KU Leuven (Belgium) in 2019. His main research interests include biopolymers, drug delivery, nanoparticles, and tissue engineering.

Ferry Melchels is associate professor in the Institute of Biological Chemistry, Biophysics and Bioengineering at Heriot-Watt University. He develops and studies polymeric biomaterials, combining hydrogels, scaffold materials, and cells with biofabrication technologies to prepare 3D constructs for regenerative medicine, in vitro modeling, and drug delivery. Ferry holds an M.Sc. (2005) in chemical engineering and Ph.D. (2010) in biomaterials from the University of Twente (The Netherlands).